

To-do list

1. Rethink	4
2. Anything wrong with standardising?	5
3. Attempt to prove this.	23

Contents

4 Regression with I-priors	3
4.1 Various regression models	4
4.1.1 Multiple linear regression	4
4.1.2 Multilevel linear modelling	5
4.1.3 Longitudinal modelling	8
4.1.4 Classification	8
4.1.5 Smoothing models	10
4.1.6 Regression with functional covariates	12
4.2 Estimation	13
4.2.1 The intercept and the prior mean	14
4.2.2 Direct optimisation	15
4.2.3 Expectation-maximisation algorithm	17
4.2.4 Markov chain Monte Carlo methods	18
4.2.5 Comparison of estimation methods	19
4.3 Computational considerations	21
4.3.1 The Nystrom approximation	21
4.3.2 Front-loading kernel matrices for the EM algorithm	23
4.3.3 The exponential family EM algorithm	27
4.4 Post-estimation	30
4.5 Examples	34
4.5.1 Using the Nystrom method	34

4.5.2	Random effects models	37
4.5.3	Longitudinal data analysis	42
4.5.4	Regression with a functional covariate	46
4.6	Conclusion	52
Bibliography		57

Haziq Jamil

Department of Statistics

London School of Economics and Political Science

PhD thesis: ‘Regression modelling using Fisher information covariance kernels (I-priors)’

Chapter 4

Regression with I-priors

chapter4

In the previous chapter, we defined an I-prior for the normal regression model (1.1) subject to (1.2) and f belonging to a reproducing kernel Hilbert or Krein space of functions \mathcal{F} , as a Gaussian distribution on f with covariance function proportional to the Fisher information for f . We also saw how new function spaces can be constructed via the polynomial and ANOVA RKKS. In this chapter, we shall describe various regression models, and identify them with appropriate RKKSs, so that an I-prior may be defined on it.

Methods for estimating I-prior models are described in Section 4.2. Estimation here refers to obtaining the posterior distribution of the regression function under an I-prior, while optimising the kernel parameters of \mathcal{F} and the error precision Ψ . Likelihood based methods, namely direct optimisation of the likelihood and the expectation-maximisation (EM) algorithm, are the preferred estimation methods of choice. Having said this, it is also possible to estimate I-prior models under a full Bayesian paradigm by employing Markov chain Monte Carlo methods to sample from the relevant posterior densities.

Careful considerations of the computational aspects are required to ensure efficient estimation of I-prior models, and these are discussed in Section 4.3. The culmination of the computational work on I-prior estimation is the **iprior** package (Jamil and Bergsma, 2017), which is a publicly available R package that has been published to CRAN.

Finally, several examples of I-prior modelling are presented in Section 4.5: in particular, a multilevel data set, a longitudinal data set, and a data set involving a functional covariate, are analysed using the I-prior methodology.

sec:various
-regression

4.1 Various regression models

In the introductory chapter (Section 1.1), we described several interesting regression models. The goal of this section is to formulate the I-prior model that describes each of these models. This is done by carefully choosing the RKHS/RKKS \mathcal{F} of real functions over a set \mathcal{X} to which the regression function f belongs. Without loss of generality and for simplicity, assume a prior mean of zero for the I-prior distribution.

4.1.1 Multiple linear regression

Let $\mathcal{X} \equiv \mathbb{R}^p$ be equipped with the regular Euclidean dot product, and \mathcal{F}_λ be the scaled canonical RKHS of functions over \mathcal{X} with kernel $h_\lambda(\mathbf{x}, \mathbf{x}') = \lambda \mathbf{x}^\top \mathbf{x}'$, for any two $\mathbf{x}, \mathbf{x}' \in \mathbb{R}^p$. Then, an I-prior on f implies that

$$\begin{aligned} f(\mathbf{x}_i) &= \sum_{j=1}^n \lambda \mathbf{x}_i^\top \mathbf{x}_j w_j \\ &= \sum_{j=1}^n \lambda \left(\sum_{k=1}^p x_{ik} x_{jk} \right) w_j \\ &= \beta_1 x_{i1} + \cdots + \beta_p x_{ip}, \end{aligned}$$

where each $\beta_k := \lambda \sum_{j=1}^n x_{jk} w_j$. This implies a multivariate normal prior distribution for the regression coefficients

$$\boldsymbol{\beta} := (\beta_1, \dots, \beta_p) \sim N_p(\mathbf{0}, \lambda^2 \mathbf{X}^\top \boldsymbol{\Psi} \mathbf{X}), \quad (4.1)$$

{eq:ipriorc
anonical}

where \mathbf{X} is the $n \times p$ design matrix for the covariates, excluding the column of ones at the beginning typically reserved for the intercept. As expected, the covariance matrix for $\boldsymbol{\beta}$ is recognised as the scaled Fisher information matrix for the regression coefficients.

If the covariates are not scaled similarly, then the values of f are incoherent—if x_1 measures weight in kilograms and x_2 height in centimetres, what measurement does $\beta_1 x_1 + \beta_2 x_2$ represent? To overcome this, one could decompose the regression function into

$$f(\mathbf{x}_i) = f_1(x_{i1}) + \cdots + f_p(x_{ip})$$

for which $f \in \mathcal{F}_\lambda \equiv \mathcal{F}_{\lambda_1} \oplus \cdots \oplus \mathcal{F}_{\lambda_p}$, and \mathcal{F}_{λ_k} , $k = 1, \dots, p$ are unidimensional canonical RKHSs with kernels $h_{\lambda_k}(x_{ik}, x_{jk}) = \lambda_k x_{ik} x_{jk}$. In effect, we now have p scale parameters,

1. Re-
think

one for each of the RKKSs associated with the p covariates. The RKKS \mathcal{F}_λ therefore has kernel

$$h(\mathbf{x}_i, \mathbf{x}_j) = \sum_{k=1}^p \lambda_k x_{ik} x_{jk},$$

and hence each regression coefficient can now be written as $\beta_k = \sum_{j=1}^n \lambda_k x_{jk} w_j$, for which we see the λ_k 's scaling role on the x_{jk} 's. Thus, the corresponding I-prior for $\boldsymbol{\beta}$ is

$$\boldsymbol{\beta} \sim N_p(\mathbf{0}, \mathbf{X}^\top \boldsymbol{\Lambda} \Psi \boldsymbol{\Lambda} \mathbf{X}),$$

with $\boldsymbol{\Lambda} = \text{diag}(\lambda_1, \dots, \lambda_p)$. Note that \mathcal{F}_λ can be seen as a special case of the ANOVA RKKS, in which only the main effects are considered, in which case the *centred canonical RKHSs* should be considered instead. This approach is disadvantageous when p is large, in which case there would be numerous scale parameters to estimate.

Remark 4.1. Of course, one could simply turn to standardisation of the \mathbf{X} variables, so as to make the variables measure on the same scale. We feel this is a rather ad-hoc approach—how can one be sure that the variables are centred and scaled appropriately? On the other hand, there is a balance to be made between elegance and feasibility. With large p , standardising is much simpler and computationally less burdensome than estimating p individual scale parameters. In [Chapter 6](#), where we tackle the problem of Bayesian variable selection using I-priors in linear models, standardisation of the variables is done for the sake of streamlining the Gibbs sampler.

Remark 4.2. The I-prior for $\boldsymbol{\beta}$ in (4.1) bears resemblance to the g -prior ([Zellner, 1986](#)), and in fact, the g -prior can be interpreted as an I-prior if the inner product of \mathcal{X} is the Mahalanobis inner product. See [Appendix E](#) for a discussion.

4.1.2 Multilevel linear modelling

Let $\mathcal{X} \equiv \mathbb{R}^p$, and suppose that alongside the covariates, there is information on group levels $\mathcal{M} = \{1, \dots, m\}$ for each unit i . That is, every observation for unit i is known to belong to a specific group j , and we write $\mathbf{x}_i^{(j)}$ to indicate this. Let n_j denote the sample size for cluster j , and the overall sample size be $n = \sum_{j=1}^m n_j$. When modelled linearly with the responses $y_i^{(j)}$, the model is known as a multilevel (linear) model, although it is known by many other names: random-effects models, random coefficient models, hierarchical models, and so on. As this model is seen as an extension of linear models,

2. Anything wrong with standardising?

sec:multilevelmodels

applications are plenty, especially in research designs for which the data varies at more than one level.

Consider a functional ANOVA decomposition of the regression function as follows:

$$f(\mathbf{x}_i^{(j)}, j) = \alpha + f_1(\mathbf{x}_i^{(j)}) + f_2(j) + f_{12}(\mathbf{x}_i^{(j)}, j). \quad (4.2)$$

{eq:anova
multilevel}

To mimic the standard linear multilevel model, assume $f_1 \in \mathcal{F}_1$ the Pearson RKHS, $f_2 \in \mathcal{F}_2$ the centred canonical RKHS, and $f_{12} \in \mathcal{F}_{12} = \mathcal{F}_1 \otimes \mathcal{F}_2$, the tensor product space of \mathcal{F}_1 and \mathcal{F}_2 . As we know, α is the overall intercept, and the varying intercepts are given by the function f_2 . While f_1 is the (main) linear effect of the covariates, f_{12} provides the varying linear effect of the covariates by each group. The I-prior for $f - \alpha$ is assumed to lie in the function space $\mathcal{F} - \alpha$, which is an ANOVA RKKS with kernel

$$h_\lambda((\mathbf{x}_i^{(j)}, j), (\mathbf{x}_{i'}^{(j')}, j')) = \lambda_1 h_1(\mathbf{x}_i^{(j)}, \mathbf{x}_{i'}^{(j')}) + \lambda_2 h_2(j, j') + \lambda_1 \lambda_2 h_1(\mathbf{x}_i^{(j)}, \mathbf{x}_{i'}^{(j')}) h_2(j, j'),$$

with h_1 the centred canonical kernel and h_2 the Pearson kernel. The reason for not including an RKHS of constant functions in \mathcal{F} is because the overall intercept is usually simpler to estimate as an external parameter (see [Section 4.2.1](#)).

We can show that the regression function (4.2) corresponds to the standard way of writing the multilevel model,

$$f(\mathbf{x}_i^{(j)}, j) = \beta_0 + \mathbf{x}_i^{(j)\top} \boldsymbol{\beta}_1 + \beta_{0j} + \mathbf{x}_i^{(j)\top} \boldsymbol{\beta}_{1j}.$$

and determine the prior distributions on $(\beta_{0j}, \boldsymbol{\beta}_{1j}^\top)^\top \in \mathbb{R}^{p+1}$. For the interested reader, the details are in [Appendix F.1](#). The standard multilevel random effects assumption is that $(\beta_{0j}, \boldsymbol{\beta}_{1j}^\top)^\top$ is normally distributed with mean zero and covariance matrix $\boldsymbol{\Phi}$. In total, there are $p + 1$ regression coefficients and $(p + 1)(p + 2)/2$ covariance parameters in $\boldsymbol{\Phi}$ to be estimated. In contrast, the I-prior model is parameterised by only two RKKS scale parameters—one for \mathcal{F}_1 and one for \mathcal{F}_2 —and the error precision ψ . While the estimation procedure for $\boldsymbol{\Phi}$ in the standard multilevel model can result in non-positive covariance matrices, the I-prior model has the advantage that positive definiteness is taken care of automatically¹.

As a remark, the following regression functions are nested

¹By virtue of the estimate of the regression function belonging to \mathcal{F}_n , an RKHS with a positive definite kernel equal to the Fisher information for f .

- $f(\mathbf{x}_i^{(j)}, j) = \alpha + f_1(\mathbf{x}_i^{(j)}) + f_2(j)$ (random intercept model);
- $f(\mathbf{x}_i^{(j)}, j) = \alpha + f_1(\mathbf{x}_i^{(j)})$ (linear regression model);
- $f(\mathbf{x}_i^{(j)}, j) = \alpha + f_2(j)$ (ANOVA model);
- $f(\mathbf{x}_i^{(j)}, j) = \alpha$ (intercept only model),

and thus one may compare likelihoods to ascertain the best fitting model. In addition, one may add flexibility to the model in two possible ways:

1. **More than two levels.** The model can be easily adjusted to reflect the fact that the data is structured in a hierarchy containing three or more levels. For the three level case, let the indices $j \in \{1, \dots, m_1\}$ and $k \in \{1, \dots, m_2\}$ denote the two levels, and simply decompose the regression function accordingly:

$$f(\mathbf{x}_i^{(j,k)}, j, k) = \alpha + f_1(\mathbf{x}_i^{(j,k)}) + f_2(j) + f_3(k) + f_{12}(\mathbf{x}_i^{(j,k)}, j) + f_{13}(\mathbf{x}_i^{(j,k)}, k) + f_{23}(j, k) + f_{123}(\mathbf{x}_i^{(j,k)}, j, k).$$

2. **Covariates not varying with levels.** Suppose now we would like to add covariates with a fixed effect to the model, i.e., covariates $\mathbf{z}_i^{(j)}$ which are not assumed to affect the responses differently in each group. The regression function would be:

$$f(\mathbf{x}_i^{(j)}, j, \mathbf{z}_j) = \alpha + f_1(\mathbf{x}_i^{(j)}) + f_2(j) + f_3(\mathbf{z}_i^{(j)}) + f_{12}(\mathbf{x}_i^{(j)}, j).$$

This can be seen as a limited functional ANOVA decomposition of f .

Remark 4.3. Indexing can be tricky, but we find the following helpful. Supposing $m = 2$, and $n_1 = n_2 = 3$, then a typical panel data set looks like this:

y	x	z	i	j	k
y_{11}	x_{11}	z_1	1	1	1
y_{21}	x_{21}	z_1	2	1	2
y_{31}	x_{31}	z_1	3	1	3
y_{12}	x_{12}	z_2	1	2	4
y_{22}	x_{22}	z_2	2	2	5
y_{32}	x_{32}	z_2	3	2	6

The y 's are the responses, x 's covariates, and z 's group-level covariates. If $\iota : (i, j) \mapsto k$ is a function which maps the dual index set (i, j) to the single index set $k \in \{1, \dots, n\}$, then the multilevel regression function can be expressed as the regression function in model (1.1).

4.1.3 Longitudinal modelling

Longitudinal or panel data observes covariate measurements $x_i \in \mathcal{X}$ and responses $y_i(t) \in \mathbb{R}$ for individuals $i = 1, \dots, n$ across a time period $t \in \{1, \dots, T\} =: \mathcal{T}$. Often, the time indexing set \mathcal{T} may be unique to each individual i , so measurements for unit i happens across a time period $\{t_{i1}, \dots, t_{iT_i}\} =: \mathcal{T}_i$ —this is known as an unbalanced panel. It is also possible that covariate measurements vary across time too, so appropriately they are denoted $x_i(t)$. For example, $x_i(t)$ could be repeated measurements of the variable x_i at time point $t \in \mathcal{T}_i$. The relationship between the response variables $y_i(t)$ at time $t \in \mathcal{T}_i$ is captured through the equation

$$y_i(t) = f(x_i, t) + \epsilon_i(t)$$

where the distribution of $\epsilon_i = (\epsilon_i(t_{i1}), \dots, \epsilon_i(t_{iT_i}))^\top$ is Gaussian with mean zero and covariance matrix Ψ_i . Assuming $\Psi_i = \psi_i \mathbf{I}_{T_i}$ or even $\Psi_i = \psi \mathbf{I}_{T_i}$ are perfectly valid choices, even though this seemingly ignores any time dependence between the observations. In reality, the I-prior induces time dependence of the observations via the kernels in the prior covariance matrix for f . Additionally, the random vectors ϵ_i and $\epsilon_{i'}$ are assumed to be independent for any two distinct $i, i' \in \{1, \dots, n\}$.

Motivated by a functional ANOVA decomposition, we obtain

$$f(x_i, t) = \alpha + f_1(i) + f_2(x_i) + f_3(t) + f_{13}(i, t) + f_{23}(x_i, t) + f_{123}(i, x_i, t), \quad (4.3)$$

{eq:longitudinalanova}

where α is an overall constant, $f_k \in \mathcal{F}_k$, $k = 1, 2, 3$, $f_{j3} \in \mathcal{F}_j \otimes \mathcal{F}_3$, $j = 1, 2$, and $f_{123} \in \mathcal{F}_1 \otimes \mathcal{F}_2 \otimes \mathcal{F}_3$. \mathcal{F}_1 is the Pearson RKHS, but choices for \mathcal{F}_2 and \mathcal{F}_3 are plentiful. In fact, any of the RKHS/RKKS described in Chapter 3 can be used to either model a linear dependence (canonical RKHS), nominal dependence (Pearson RKHS), polynomial dependence (polynomial RKKS) or smooth dependence (fBm or SE RKHS) on the x_i 's and t 's on f .

4.1.4 Classification

We describe a naïve classification model using I-priors. Here, the responses are categorical $y_i \in \{1, \dots, m\} =: \mathcal{M}$, and additionally, write $\mathbf{y}_i. = (y_{i1}, \dots, y_{im})^\top$ where the class responses y_{ij} equal one if individual i 's response category is $y_i = j$, and zero otherwise. In other words, there is exactly a single '1' at the j 'th position in the vector $\mathbf{y}_i.$, and

zeroes everywhere else. For $j = 1, \dots, m$, we model

$$y_{ij} = \alpha + \overbrace{\alpha_j + f_j(x_i)}^{f(x_{i,j})} + \epsilon_{ij} \quad (4.4)$$

$$(\epsilon_{i1}, \dots, \epsilon_{im})^\top \stackrel{\text{iid}}{\sim} N_m(\mathbf{0}, \Psi^{-1}).$$

{eq:naiveclassmod}

The idea here being that we attempt to model the class responses y_{ij} using class-specific regression functions f_j , and the class responses are assumed to be independent among individuals, but may or may not be correlated among classes for each individual. The class correlations are manifest themselves in the variance of the errors Ψ^{-1} , which is an $m \times m$ matrix.

Denote the regression function f in (4.4) on the set $\mathcal{X} \times \mathcal{M}$ as $f(x_i, j) = \alpha_j + f_j(x_i)$. This regression function corresponds to an ANOVA decomposition of the spaces $\mathcal{F}_{\mathcal{M}}$ and $\mathcal{F}_{\mathcal{X}}$ of functions over \mathcal{M} and \mathcal{X} respectively. That is, $\mathcal{F} = \mathcal{F}_{\mathcal{M}} \oplus (\mathcal{F}_{\mathcal{M}} \otimes \mathcal{F}_{\mathcal{X}})$ is a decomposition into the main effects of ‘class’, and an interaction effect of the covariates for each class. Let $\mathcal{F}_{\mathcal{M}}$ and $\mathcal{F}_{\mathcal{X}}$ be RKHSs respectively with kernels $a : \mathcal{M} \times \mathcal{M} \rightarrow \mathbb{R}$ and $b_\eta : \mathcal{X} \times \mathcal{X} \rightarrow \mathbb{R}$. Then, the ANOVA RKKS \mathcal{F} possesses the reproducing kernel $h_\eta : (\mathcal{X} \times \mathcal{M})^2 \rightarrow \mathbb{R}$ as defined by

$$h_\eta((x, j), (x', j')) = a(j, j') + a(j, j')b_\eta(x, x'). \quad (4.5)$$

{eq:anovaclass}

The kernel b_η may be any of the kernels described in this thesis, ranging from the linear kernel, to the fBm kernel, or even an ANOVA kernel. Choices for $a : \mathcal{M} \times \mathcal{M} \rightarrow \mathbb{R}$ include

1. **The Pearson kernel** (as defined in Definition 2.34). With $J \sim P$, a probability measure over \mathcal{M} ,

$$a(j, j') = \frac{\delta_{jj'}}{P(J = j)} - 1.$$

2. **The centred identity kernel**. With δ denoting the Kronecker delta function,

$$a(j, j') = \delta_{jj'} - 1/m.$$

The purpose of either of these kernels is to contribute to the class intercepts α_j , and to associate a regression function in each class. The only difference between the two is the inverse probability weighting per class that is applied in the Pearson kernel, but not in the identity kernel.

With $f \in \mathcal{F}$ (the RKKS with kernel h_η), it is straightforward to assign an I-prior on f . It is in fact

$$f(x_i, j) = \sum_{j'=1}^m \sum_{i'=1}^n a(j, j')(1 + b_\eta(x_i, x_{i'}))w_{i'j'} \quad (4.6)$$

$$(w_{i'1}, \dots, w_{i'm})^\top \stackrel{\text{iid}}{\sim} N_m(\mathbf{0}, \Psi)$$

{eq:naiveclassificationprior}

assuming a zero prior mean $f_0(x, j) = 0$. The model then classifies the i 'th data point to class j if $\hat{y}_{ij} = \max(\hat{y}_{i1}, \dots, \hat{y}_{im})$, where $\hat{y}_{ik} = \hat{\alpha} + \hat{f}(x_i, k)$, the prediction for the k 'th component of y_i .

There are several downfalls to using the model described above. Unlike in the case of continuous response variables, the normal I-prior model is highly inappropriate for categorical responses. For one, it violates the normality and homoscedasticity assumptions of the errors. For another, predicted values may be out of the range $[0, m]$ and thus poorly calibrated. Furthermore, it would be more suitable if the class probabilities—the probability of an observation belonging to a particular class—were also part of the model. In [Chapter 5](#), we propose an improvement to this naïve I-prior classification model by considering a probit-like transformation of the regression functions.

4.1.5 Smoothing models

Single- and multi-variable smoothing models can be fitted under the I-prior methodology using the fBm RKHS. In standard kernel based smoothing methods, the squared exponential kernel is often used, and the corresponding RKHS contains analytic functions. There are several attractive properties of using the fBm RKHS, and for one-dimensional smoothing, these are discussed below.

Assume that, up to a constant, the regression function lies in the scaled, centred fBm RKHS \mathcal{F} of functions over $\mathcal{X} \equiv \mathbb{R}$ with Hurst index $1/2$. Thus, with a centring with respect to the empirical distribution P_n of $\{x_1, \dots, x_n\}$ and using the absolute norm on \mathbb{R} , \mathcal{F} has kernel

$$h_\lambda(x, x') = \frac{\lambda}{2n^2} \sum_{i=1}^n \sum_{j=1}^n (|x - x_i| + |x' - x_j| - |x - x'| - |x_i - x_j|).$$

As proven by [van der Vaart and van Zanten \(2008, Section 10\)](#), \mathcal{F} contains absolutely continuous functions possessing a square integrable weak derivative satisfying $f(0) = 0$.

The norm is given by $\|f\|_{\mathcal{F}}^2 = \int f^2 dx$. The posterior mean of f based on an I-prior is then a (one-dimensional) smoother for the data. For f of the form $f = \sum_{i=1}^n h(\cdot, x_i) w_i$, i.e., $f \in \mathcal{F}_n$, the finite subspace of \mathcal{F} as in [Section 3.4](#), then [Bergsma \(2017\)](#) shows that f can be represented as

$$f(x) = \int_{-\infty}^x \beta(t) dt \quad (4.7)$$

where

$$\beta(t) = \sum_{i: x_i \leq t} w_i = \frac{f(x_{i_t+1}) - f(x_{i_t})}{x_{i_t+1} - x_{i_t}} \quad (4.8)$$

with $i_t = \max_{x_i \leq t} i$. Under the I-prior with an iid assumption on the errors, the w_i 's are zero mean normal random variables with variance ψ , so that β as defined above is an ordinary Brownian bridge with respect to the empirical distribution P_n . The I-prior for f is piecewise linear with knots at x_1, \dots, x_n , and the same holds true for the posterior mean. The implication is that the I-prior automatically adapts to irregularly spaced x_i : in any region where there are no observations, the resulting smoother is linear. This is explained by the reduced Fisher information about the derivative of the regression curve in regions with no observation.

In [Bergsma \(2017\)](#), it is shown that the covariance function for β is

$$\text{Cov} [\beta(x), \beta(x')] = n (\min\{P_n(X < x), P_n(X_n < x')\} - P_n(X < x) P_n(X_n < x'))$$

From this, notice that $\text{Var}[\beta(x)] = P_n(X_n < x)(1 - P_n(X_n < x))$, which shows an automatic boundary correction: close to the boundary there is little Fisher information on the derivative of the regression function $\beta(x)$, so the prior variance is small. This will lead to more shrinkage of the posterior derivative of f towards the derivative of the prior mean f_0 .

Another advantage of the I-prior methodology is the ability to fit single or multi-dimensional smoothing models with just two parameters to be estimated: the RKHS scale parameter λ and the error precision Ψ . The Hurst parameter $\gamma \in (0, 1)$ of the fBm RKHS can also be treated as a free parameter for added flexibility, but for most practical applications, we find that the default setting of $\gamma = 1/2$ performs sufficiently well.

{eq:ipriorb
rownianbrid
ge}

Remark 4.4. From (4.7), the prior process for f is thus an integrated Brownian bridge. This shows a close relation with cubic spline smoothers, which can be interpreted as the posterior mean when the prior is an integrated Wiener process (Wahba, 1990). Unlike I-priors however, cubic spline smoothers do not have automatic boundary corrections, and typically the additional assumption is made that the smoothing curve is linear at the boundary knots.

4.1.6 Regression with functional covariates

Suppose that we have functional covariates x in the real domain, and that \mathcal{X} is a set of differentiable functions. If so, it is reasonable to assume that \mathcal{X} is a Hilbert-Sobolev space with inner product

$$\langle x, x' \rangle_{\mathcal{X}} = \int \dot{x}(t) \dot{x}'(t) dt,$$

so that we may apply the linear, fBm or any other kernels which make use of inner products by making use of the polarisation identity. Furthermore, let $z \in \mathbb{R}^T$ be the discretised realisation of the function $x \in \mathcal{X}$ at regular intervals $t = 1, \dots, T$. Then

$$\langle x, x' \rangle_{\mathcal{X}} \approx \sum_{t=1}^{T-1} (z_{t+1} - z_t)(z'_{t+1} - z'_t).$$

For discretised observations at non-regular intervals $\{t_1, \dots, t_T\}$ then a more general formula to the above one might be used, for instance,

$$\langle x, x' \rangle_{\mathcal{X}} \approx \sum_{i=1}^{T-1} \frac{(z_{t_{i+1}} - z_{t_i})(z'_{t_{i+1}} - z'_{t_i})}{t_{i+1} - t_i}.$$

sec:regfunc
tionalcov

sec:ipriore
stimation

4.2 Estimation

After selecting a RKHS/RKKS \mathcal{F} of functions over \mathcal{X} suitable for the regression problem at hand, one then proceeds to estimate the posterior distribution of the regression function. The I-prior model (1.1) subject to (1.2) and $f \in \mathcal{F}$ has the simple and convenient representation

$$\begin{aligned}
 y_i &= \alpha + \overbrace{f_0(x_i)}^{f(x_i)} + \sum_{k=1}^n h_\eta(x_i, x_k) w_k + \epsilon_i \\
 (\epsilon_1, \dots, \epsilon_n)^\top &\sim \mathcal{N}_n(\mathbf{0}, \Psi^{-1}) \\
 (w_1, \dots, w_n)^\top &\sim \mathcal{N}_n(\mathbf{0}, \Psi),
 \end{aligned} \tag{4.9}$$

{eq:model2}

where $f_0 : \mathcal{X} \rightarrow \mathbb{R}$ is a function chosen a priori representing the ‘best guess’ of f , and the dependence of the kernel of \mathcal{F} on parameters η is emphasised through the subscript in $h_\eta : \mathcal{X} \times \mathcal{X} \rightarrow \mathbb{R}$.

The parameters of the I-prior model are collectively denoted by $\theta = \{\alpha, \eta, \Psi\}$. Given θ and a prior choice for f_0 , the posterior regression function is determined solely by the posterior distribution of the w_i ’s. Using standard multivariate normal results, one finds that the posterior distribution for $\mathbf{w} := (w_1, \dots, w_n)^\top$ is $\mathbf{w}|\mathbf{y} \sim \mathcal{N}_n(\tilde{\mathbf{w}}, \tilde{\mathbf{V}}_w)$, where

$$\tilde{\mathbf{w}} = \Psi \mathbf{H}_\eta \mathbf{V}_y^{-1} (\mathbf{y} - \alpha \mathbf{1}_n - \mathbf{f}_0) \quad \text{and} \quad \tilde{\mathbf{V}}_w = (\mathbf{H}_\eta \Psi \mathbf{H}_\eta + \Psi^{-1})^{-1} = \mathbf{V}_y^{-1}, \tag{4.10}$$

{eq:posteriorw}

using the familiar notation that we introduced in [Section 1.4](#). For a derivation, see [Appendix G.1](#). By linearity, the posterior distribution for f is also normal.

In each modelling scenario, there are a number of kernel parameters η that need to be estimated from the data. Assuming that the covariate space is $\mathcal{X} = \mathcal{X}_1 \times \dots \times \mathcal{X}_p$, and there is an ANOVA like decomposition of the function space \mathcal{F} into its constituents spaces $\mathcal{F}_1, \dots, \mathcal{F}_p$, then at the very least, there are p scale parameters $\lambda_1, \dots, \lambda_p$ for each of the RKHSs. Depending on the RKHS used, there could be more kernel parameters that need to be optimised, for instance, the Hurst index for the fBm RKHS, the lengthscale for the SE RKHS, and/or the offset for the polynomial RKKS. However, these may be treated as fixed parameters as well.

The following subsections describe possible estimation procedures for the hyperparameters of the model. Henceforth, for simplicity, the following additional standing assumptions are imposed on the I-prior model (4.9):

A1 Centred responses. Set $\alpha = 0$ and replace the responses by their centred versions

$$y_i \mapsto \tilde{y}_i = y_i - \frac{1}{n} \sum_{i=1}^n y_i.$$

A2 Zero prior mean. Assume a zero prior mean $f_0(x) = 0$ for all $x \in \mathcal{X}$.

A3 Iid errors. Assume identical and independent (iid) errors random variables, i.e., $\Psi = \psi \mathbf{I}_n$.

Assumptions A1 and A2 are motivated by the discussion in Section 4.2.1. Although assumption A3 is not strictly necessary, it is often a reasonable one and one that simplifies the estimation procedure greatly.

4.2.1 The intercept and the prior mean

In most statistical models, an intercept is a necessary inclusion which aids interpretation. In the context of the I-prior model (4.9), a lack of an intercept would fail to account for the correct locational shift of the regression function along the y -axis. Further, when zero-mean functions are considered, the intercept serves as being the ‘grand mean’ value of the responses.

The handling of an intercept to the regression model may be viewed in one of two ways. The first is to view it as a function belonging to the RKHS of constant functions \mathcal{F}_0 , and thereby tensor summing this space to \mathcal{F} . The second is to simply treat the intercept as a parameter of the model to be estimated. In the polynomial and ANOVA RKKSs, we saw that an intercept is naturally induced by the inclusion of a RKHS of constant functions in their construction. In any of the other RKHSs described in Chapter 2, an intercept would need to be added separately. These two methods convey slightly different interpretations of the intercept: in the first method, the intercept is shrunk by an I-prior, while in the second, it is not. Estimation is also entirely different for the two methods.

In the first method, the intercept-less RKHS/RKKS \mathcal{F} with kernel h is made to include an intercept by modifying the kernel to be $h + 1$. The intercept will then be implicitly taken care of without having dealt with it explicitly. However, it can be obtained by realising that for $\alpha \in \mathcal{F}_0$ the RKHS of constant functions, then $\alpha = \sum_{i=1}^n w_i$.

On the other hand, consider the intercept as a parameter α to be estimated. Obtaining an estimate α using a likelihood-based argument is rather simple. From (4.9), $E[y_i] = \alpha + f_0(x_i)$ for all $i = 1, \dots, n$, so the maximum likelihood estimate for $E y$ is its sample mean $\bar{y} = \frac{1}{n} \sum_{i=1}^n y_i$, and hence the ML estimate for α is $\hat{\alpha} = \bar{y} - \frac{1}{n} \sum_{i=1}^n f_0(x_i)$.

Finally, the estimation of α under a fully Bayesian treatment is possible by assuming an appropriate hyperprior on it, such as a conjugate normal prior $N(a, A^{-1})$. If so, the conditional posterior of α given \mathbf{w} , η , Ψ and f_0 is also normal with mean \tilde{a} and variance \tilde{A} , where

$$\tilde{A} = \sum_{i,j=1}^n \psi_{ij} + A \quad \text{and} \quad \tilde{a} = \tilde{A}^{-1} \left(\sum_{i=1}^n [(\mathbf{y} - \mathbf{f}_0 - \mathbf{H}_\eta \mathbf{w}) \Psi]_i + Aa \right).$$

This fact can be used, say, in conjunction with a Gibbs sampling procedure treating the rest of the unknowns as random. Note that the posterior mean for α is

$$E[\alpha|\mathbf{y}] = E_{\mathbf{w}} [E[\alpha|\mathbf{y}, \mathbf{w}]] = \frac{\sum_{i,j=1}^n \psi_{ij}(y_i - f_0(x_i)) + Aa}{\sum_{i,j=1}^n \psi_{ij} + A},$$

which, in the iid errors case, is seen to be a weighted sum of the ML estimate $\hat{\alpha}$ and the prior mean a . Unless there is a strong reason to add prior information to the intercept, the ML estimate seems to be the simplest approach. Assumption A1 therefore implies a ML estimation of the intercept parameter.

4.2.2 Direct optimisation

Under assumptions A1–A3, a direct optimisation of the parameters $\theta = \{\eta, \Psi = \psi \mathbf{I}_n\}$ using the log-likelihood of θ is straightforward to implement. Denote $\Sigma_\theta := \psi \mathbf{H}_\eta^2 + \psi^{-1} \mathbf{I}_n = \mathbf{V}_y$. From (4.9), the (marginal) log-likelihood of θ is given by

$$\begin{aligned} L(\theta) &= \log \int p(\mathbf{y}|\mathbf{w}, \theta) p(\mathbf{w}|\theta) d\mathbf{w} \\ &= -\frac{n}{2} \log 2\pi - \frac{1}{2} \log |\Sigma_\theta| - \frac{1}{2} \tilde{\mathbf{y}}^\top \Sigma_\theta^{-1} \tilde{\mathbf{y}}. \end{aligned} \tag{4.11}$$

{eq:marglog
liky}

The term marginal refers to the fact that we are averaging out the random function represented by \mathbf{w} . Direct optimisation is typically done using conjugate gradients with a Cholesky decomposition on the covariance kernel to maintain stability, but we opt for an eigendecomposition of the kernel matrix $\mathbf{H}_\eta = \mathbf{V} \text{diag}(u_1, \dots, u_n) \mathbf{V}^\top$ instead. Further,

since \mathbf{H}_η is a symmetric matrix, we have that $\mathbf{V}\mathbf{V}^\top = \mathbf{I}_n$, and thus

$$\begin{aligned}\mathbf{V}_y &= \psi \mathbf{V} \text{diag}(u_1^2, \dots, u_n^2) \mathbf{V}^\top + \psi^{-1} \mathbf{V}\mathbf{V}^\top \\ &= \mathbf{V} \text{diag}(\psi u_1^2 + \psi^{-1}, \dots, \psi u_n^2 + \psi^{-1}) \mathbf{V}^\top\end{aligned}$$

for which the inverse and log-determinant is easily obtainable. To be explicit, the log-likelihood is given by

$$\begin{aligned}L(\theta) &= -\frac{n}{2} \log 2\pi - \frac{1}{2} \sum_{i=1}^n \log(\psi u_i^2 + \psi^{-1}) \\ &\quad - \frac{1}{2} \tilde{\mathbf{y}}^\top \mathbf{V} \text{diag}\left(\frac{1}{\psi u_1^2 + \psi^{-1}}, \dots, \frac{1}{\psi u_n^2 + \psi^{-1}}\right) \mathbf{V}^\top \tilde{\mathbf{y}}\end{aligned}\tag{4.12}$$

This method is relatively robust to numerical instabilities and is better at ensuring positive definiteness of the covariance kernel. The direct optimisation method can be prone to local optima, in which case repeating the optimisation at different starting points and choosing the one which yields the highest likelihood is one way around this. On a practical note, parameters are best transformed so that optimisation of these parameters are done on an unrestricted scale (e.g. $\log \psi$).

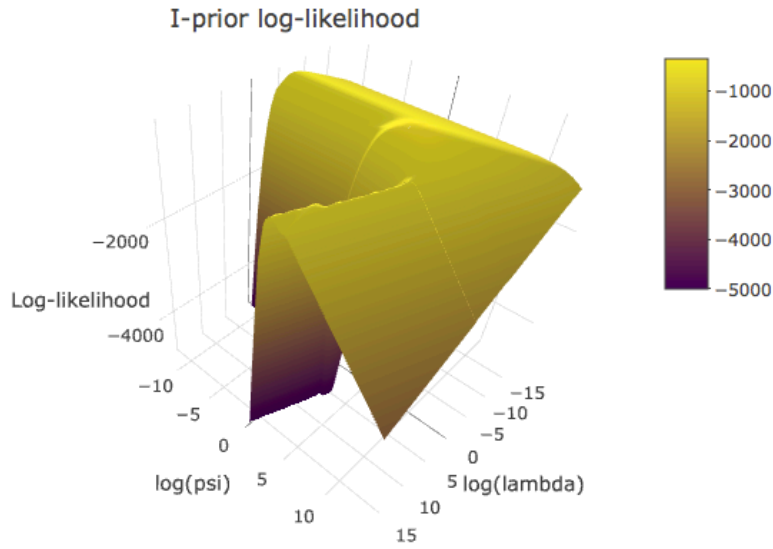


Figure 4.1: A typical log-likelihood surface plot of I-prior models, in which there are two ridges. The maximum occurs along one of the two ridges, or sometimes at the intersection. Clearly, different initialisations can lead optimisation algorithms to either ridge and possibly converge to a local optima.

Let \mathbf{U} be the Fisher information matrix for $\theta \in \mathbb{R}^q$. Standard calculations (Appendix C.1) show that under the marginal distribution $\tilde{\mathbf{y}} \sim N_n(\mathbf{0}, \Sigma_\theta)$, the (i, j) 'th coordinate of \mathbf{U} is

$$u_{ij} = \frac{1}{2} \text{tr} \left(\Sigma_\theta^{-1} \frac{\partial \Sigma_\theta}{\partial \theta_i} \Sigma_\theta^{-1} \frac{\partial \Sigma_\theta}{\partial \theta_j} \right), \quad i, j = 1, \dots, q, \quad (4.13)$$

where the derivative of a matrix with respect to a scalar is the element-wise derivative of the matrix. With $\hat{\theta}$ denoting the ML estimate for θ , under suitable conditions, $\sqrt{n}(\hat{\theta} - \theta)$ has an asymptotic multivariate normal distribution with mean zero and covariance matrix \mathbf{U}^{-1} (Casella and Berger, 2002). In particular, the standard error for θ_k is the k 'th diagonal element of $\mathbf{U}^{-1/2}$.

4.2.3 Expectation-maximisation algorithm

Evidently, the model in (4.9) resembles a random-effects model, for which the EM algorithm is easily employed to estimate its hyperparameters. Assume A1–A3 holds. By treating the complete data as $\{\mathbf{y}, \mathbf{w}\}$ and the w_i 's as “missing”, the t 'th iteration of the E-step entails computing

$$\begin{aligned} Q(\theta) &= E_{\mathbf{w}} \left[\log p(\mathbf{y}, \mathbf{w} | \theta) \mid \mathbf{y}, \theta^{(t)} \right] \\ &= E_{\mathbf{w}} \left[\text{const.} + \frac{n}{2} \log \psi - \frac{\psi}{2} \|\tilde{\mathbf{y}} - \mathbf{H}_\eta \mathbf{w}\|^2 - \frac{n}{2} \log \psi - \frac{\psi^{-1}}{2} \|\mathbf{w}\|^2 \mid \mathbf{y}, \theta^{(t)} \right] \\ &= \text{const.} - \frac{\psi}{2} \tilde{\mathbf{y}}^\top \tilde{\mathbf{y}} - \frac{1}{2} \text{tr} \left(\overbrace{(\psi \mathbf{H}_\eta^2 + \psi^{-1} \mathbf{I}_n)}^{\Sigma_\theta} \tilde{\mathbf{W}}^{(t)} \right) + \psi \tilde{\mathbf{y}}^\top \mathbf{H}_\eta \tilde{\mathbf{w}}^{(t)}, \end{aligned} \quad (4.14)$$

{eq:QfnEstep}

where $\tilde{\mathbf{w}}^{(t)} = E[\mathbf{w} | \mathbf{y}, \theta^{(t)}]$ and $\tilde{\mathbf{W}}^{(t)} = E[\mathbf{w} \mathbf{w}^\top | \mathbf{y}, \theta^{(t)}]$ are the first and second posterior moments of \mathbf{w} calculated at the t th EM iteration. These can be computed directly from (4.10), substituting for $\theta^{(t)} = \{\eta^{(t)}, \psi^{(t)}\}$ as appropriate.

The M-step assigns $\theta^{(t+1)}$ the value of θ which maximises the Q function above. This boils down to solving the first order conditions

$$\frac{\partial Q}{\partial \eta} = -\frac{1}{2} \text{tr} \left(\frac{\partial \Sigma_\theta}{\partial \eta} \tilde{\mathbf{W}}^{(t)} \right) + \psi \tilde{\mathbf{y}}^\top \frac{\partial \mathbf{H}_\eta}{\partial \eta} \tilde{\mathbf{w}}^{(t)} \quad (4.15)$$

{eq:emtheta}

$$\frac{\partial Q}{\partial \psi} = -\frac{1}{2} \tilde{\mathbf{y}}^\top \tilde{\mathbf{y}} - \text{tr} \left(\frac{\partial \Sigma_\theta}{\partial \psi} \tilde{\mathbf{W}}^{(t)} \right) + \tilde{\mathbf{y}}^\top \mathbf{H}_\eta \tilde{\mathbf{w}}^{(t)} \quad (4.16)$$

{eq:empsi}

equated to zero. As $\partial \Sigma_\theta / \partial \psi = \mathbf{H}_\eta^2 - \psi^{-2} \mathbf{I}_n$, the solution to (4.16) for ψ admits a closed form given values for η :

$$\psi^{(t+1)} = \left\{ \frac{\text{tr } \tilde{\mathbf{W}}^{(t)}}{\tilde{\mathbf{y}}^\top \tilde{\mathbf{y}} + \text{tr}(\mathbf{H}_\eta^2 \tilde{\mathbf{W}}^{(t)}) - 2\tilde{\mathbf{y}}^\top \mathbf{H}_\eta \tilde{\mathbf{w}}^{(t)}} \right\}^{1/2}. \quad (4.17)$$

{eq:closedf
ormpsi}

We use this fact to form a sequential updating scheme $\eta^{(t)} \rightarrow \psi^{(t+1)} \rightarrow \eta^{(t+1)} \rightarrow \dots$, and this form of the EM algorithm is known as the *expectation conditional maximisation* algorithm (Meng and Rubin, 1993). Now, the solution to (4.15) can also be found in closed-form given values ψ , for many models, but in general, this is not the case. In cases where closed-form solutions do exist for η , then it is just a matter of iterating the update equations until a suitable convergence criterion is met (e.g. no more sizeable increase in successive log-likelihood values). In cases where closed-form solutions do not exist for η , the Q function is again optimised with respect to η using the gradient-based algorithms.

In our experience, the EM algorithm is more stable than direct maximisation, in the sense that the EM steps increase the likelihood in a gentle manner that prevents sudden explosions of the likelihood. In contrast, the search direction using gradient-based methods can grow the likelihood too quickly and potentially causes numerical errors to creep in. As such, the EM is especially suitable if there are many scale parameters to estimate, but on the flip side, it is typically slow to converge. The **iprior** package provides a method to automatically switch to the direct optimisation method after running several EM iterations. This then combines the stability of the EM with the speed of direct optimisation.

4.2.4 Markov chain Monte Carlo methods

For completeness, it should be mentioned that a full Bayesian treatment of the model is possible, with additional priors on the set of hyperparameters. Markov chain Monte Carlo (MCMC) methods can then be employed to sample from the posteriors of the hyperparameters, with point estimates obtained using the posterior mean or mode, for instance. Additionally, the posterior distribution encapsulates the uncertainty about the parameter, for which inference can be made. Posterior sampling can be done using Gibbs-based methods in **WinBUGS** (Lunn et al., 2000) or **JAGS** (Plummer, 2003), and both have interfaces to R via **R2WinBUGS** (Sturtz et al., 2005) and **runjags** (Denwood,

2016) respectively. Hamiltonian Monte Carlo (HMC) sampling is also a possibility, and the Stan project (Carpenter et al., 2017) together with the package **rstan** (Stan Development Team, 2016) makes this possible in R.

On the software side, all of these MCMC packages require the user to code the model individually, and we are not aware of the existence of MCMC-based packages which are able to estimate GPR models. This makes it inconvenient for GPR and I-prior models, because in addition to the model itself, the kernel functions need to be coded as well and ensuring computational efficiency would be a difficult task.

Speaking of efficiency, it is more advantageous to marginalise the I-prior and work with the marginal model (4.11), rather than the hierarchical specification (4.9). The reason for this is that the latter model has a parameter space whose dimension is $O(n)$, while the former only samples the hyperparameters. Note that the marginal model (4.11) cannot then be sampled efficiently using a Gibbs procedure as the Gibbs conditionals are not of closed-form. Instead, Hamiltonian MC should be used, which does not depend on model conjugacy.

4.2.5 Comparison of estimation methods

Consider a one-dimensional smoothing example, for which $n = 150$ data pairs (y_i, x_i) have been generated according to the relationship

$$y_i = \text{const.} + \overbrace{0.35 \phi(x_i|1, 0.8^2) + 0.65 \phi(x_i|4, 1.5^2) + \mathbf{1}(x_i > 4.5) e^{1.25(x_i-4.5)}}^{f_{\text{true}}(x_i)} + \epsilon_i, \quad (4.18)$$

where $\phi(\cdot|\mu, \sigma^2)$ is the probability density function of a normal distribution with mean μ and variance σ^2 . The observed y_i 's are thought to be noisy versions of the true points, in which ϵ_i follows an indscript, not necessarily normal, distribution. The predictors x_1, \dots, x_n have been sampled roughly from the interval $(-1, 6)$, and the sampling was intentionally not uniform so that there is slight sparsity in the middle. Figure 4.2 plots the sampled points and the true regression function.

We attempt to estimate f_{true} by a function f belonging to the fBm-0.5 RKHS \mathcal{F}_λ , with an I-prior on f . There are two parameters that need to be estimated: the scale parameter λ for the fBm-0.5 RKHS, and the error precision ψ . These can be estimated using the maximum likelihood methods described above, namely by direct optimisation using a

sec:compare
estimation

{eq:example
smoothingda
ta}

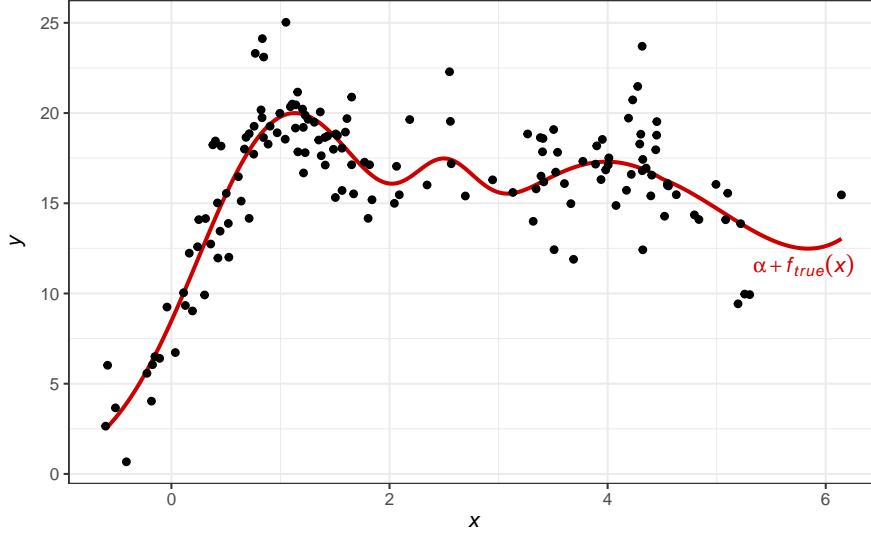


Figure 4.2: A plot of the sampled data points according to equation (4.18), with the true regression function superimposed.

fig:example
smoothingda
ta

quasi-Newton algorithm, and the EM algorithm. These two methods are implemented in the **iprior** package. A full Bayesian treatment is possible, and we use the **rstan** implementation of Stan to perform Hamiltonian Monte Carlo sampling of the posterior densities. A vague prior choice for λ and ψ are prescribed, namely

$$\lambda, \psi \stackrel{\text{iid}}{\sim} N_+(0, 100),$$

where $N_+(\mu, \sigma^2)$ represents the *half-normal* distribution². We have also set an improper prior density $p(\alpha) \propto \text{const.}$ for the intercept. The advantage of HMC is that efficiency is not dictated by conjugacy, so there is freedom to choose any appropriate prior choice on the parameters.

Table 4.1 tabulates the estimated parameter values, (marginal) log-likelihood values, and also time taken for the three estimation methods. The three methods concur on the estimated parameter values, although the scale parameter has been estimated slightly differently, which is possibly attributed to the effect of the prior for λ . The resulting log-likelihood value for the Bayesian method is lower than the ML methods, which also took the longest to compute. Although the EM algorithm took longer than the direct optimisation method to compute, the time taken per iteration is significantly shorter than one Newton iteration.

²The random variable $X \sim N_+(\mu, \sigma^2)$ has the density $p(x) = \phi(x|\mu, \sigma^2) \mathbb{1}(x \geq 0)$.

tab:compare
methodsesti
mate

Table 4.1: Table comparing the estimated parameter values, (marginal) log-likelihood values, and also time taken for the three estimation methods.

	Direct optimisation	EM algorithm	Hamiltonian MC
Intercept (α)	16.1 (0.35)	16.1 (0.35)	16.1 (0.17)
Scale (λ)	5.01 (1.23)	5.01 (1.26)	5.61 (1.42)
Precision (ψ)	0.236 (0.03)	0.236 (0.03)	0.237 (0.03)
Log density	-339.7	-339.7	-341.1
Predictive RMSE	0.574	0.575	0.582
Iterations	12	266	2000
Time taken (s)	0.96	3.65	232

sec:ipriorc
ompcons

4.3 Computational considerations

Computational complexity for estimating I-prior models (and in fact, for GPR in general) is dominated by the inversion (by way of eigendecomposition in our case) of the $n \times n$ matrix $\Sigma_\theta = \psi \mathbf{H}_\eta^2 + \psi^{-1} \mathbf{I}_n$, which scales as $O(n^3)$ in time. For the direct optimisation method, this matrix inversion is called when computing the log-likelihood, and thus must be computed at each Newton step. For the EM algorithm, this matrix inversion appears when calculating $\tilde{\mathbf{w}}$ and $\tilde{\mathbf{W}}$, the first and second posterior moments of the I-prior random effects. Furthermore, storage requirements for I-priors models are similar to that of GPR models, which is $O(n^2)$.

4.3.1 The Nyström approximation

The shared computational issues of I-prior and GPR models allow us to delve into machine learning literature, which is rich in ways to resolve these issue, as summarised by [Quiñonero-Candela and Rasmussen \(2005\)](#). One such method is to exploit low rank structures of kernel matrices. The idea is as follows. Let \mathbf{Q} be a matrix with rank $q < n$, and suppose that $\mathbf{Q}\mathbf{Q}^\top$ can be used sufficiently well to represent the kernel matrix \mathbf{H}_η . Then

$$(\psi \mathbf{H}_\eta^2 + \psi^{-1} \mathbf{I}_n)^{-1} \approx \psi \left[\mathbf{I}_n - \mathbf{Q} \left((\psi^2 \mathbf{Q}^\top \mathbf{Q})^{-1} + \mathbf{Q}^\top \mathbf{Q} \right)^{-1} \mathbf{Q}^\top \right],$$

obtained via the Woodbury matrix identity, is potentially a much cheaper operation which scales $O(nq^2)$: $O(q^3)$ to do the inversion, and $O(nq)$ to do the multiplication (because typically the inverse is premultiplied to a vector). When using the linear kernel

for a low-dimensional covariate then the above method is exact ($\mathbf{Q} = \mathbf{X}$, where \mathbf{X} is the design matrix). This fact is clearly demonstrated by the equivalence of the p -dimensional linear model implied by (4.1) with the n -dimensional I-prior model using the canonical RKHS. If $p \ll n$ then certainly using the linear representation is much more efficient.

However, other interesting kernels such as the fractional Brownian motion (fBm) kernel or the squared exponential kernel results in kernel matrices which are full rank. An approximation to the kernel matrix using a low-rank matrix is the Nyström method (Williams and Seeger, 2001). The theory has its roots in approximating eigenfunctions, but this has since been adopted to speed up kernel machines. The main idea is to obtain an (approximation to the true) eigendecomposition of \mathbf{H}_η based on a small subset $q \ll n$ of the data points.

Let $\mathbf{H}_\eta = \mathbf{V}\mathbf{U}\mathbf{V}^\top = \sum_{i=1}^n u_i \mathbf{v}_i \mathbf{v}_i^\top$ be the (orthogonal) decomposition of the symmetric matrix \mathbf{H}_η . As mentioned, avoiding this expensive $O(n^3)$ eigendecomposition is desired, and this is achieved by selecting a subset \mathcal{Q} of size q of the n data points $\{1, \dots, n\}$, so that \mathbf{H}_η may be approximated using the rank q matrix $\mathbf{H}_\eta \approx \sum_{i \in \mathcal{Q}} \tilde{u}_i \tilde{\mathbf{v}}_i \tilde{\mathbf{v}}_i^\top$. Without loss of generality, reorder the rows and columns of \mathbf{H}_η so that the data points indexed by \mathcal{M} are used first:

$$\mathbf{H}_\eta = \begin{pmatrix} \mathbf{A}_{q \times q} & \mathbf{B}_{q \times (n-q)} \\ \mathbf{B}_{q \times (n-q)}^\top & \mathbf{C}_{(n-q) \times (n-q)} \end{pmatrix}.$$

In other words, the data points indexed by \mathcal{Q} forms the smaller $q \times q$ kernel matrix \mathbf{A} . Let $\mathbf{A} = \mathbf{V}_q \mathbf{U}_q \mathbf{V}_q^\top = \sum_{i=1}^q u_i^{(q)} \mathbf{v}_i^{(q)} \mathbf{v}_i^{(q)\top}$ be the eigendecomposition of \mathbf{A} . The Nyström method provides the formulae for \tilde{u}_i and $\tilde{\mathbf{v}}_i$ (Rasmussen and Williams, 2006, §8.1, equations 8.2 and 8.3) as

$$\begin{aligned} \tilde{u}_i &:= \frac{n}{q} u_i^{(q)} \in \mathbb{R} \\ \tilde{\mathbf{v}}_i &:= \sqrt{\frac{q}{n}} \frac{1}{u_i^{(q)}} \begin{pmatrix} \mathbf{A} & \mathbf{B} \end{pmatrix}^\top \mathbf{v}_i^{(q)} \in \mathbb{R}^n. \end{aligned}$$

Denoting \mathbf{U}_q as the diagonal matrix of eigenvalues $u_1^{(q)}, \dots, u_m^{(q)}$, and \mathbf{V}_q the corresponding matrix of eigenvectors $\mathbf{v}_i^{(q)}$, we have

$$\mathbf{H}_\eta \approx \overbrace{\begin{pmatrix} \mathbf{V}_q \\ \mathbf{B}^\top \mathbf{V}_q \mathbf{U}_q^{-1} \end{pmatrix}}^{\tilde{\mathbf{V}}} \mathbf{U}_q \overbrace{\begin{pmatrix} \mathbf{V}_q^\top & \mathbf{U}_q^{-1} \mathbf{V}_q^\top \mathbf{B} \end{pmatrix}}^{\tilde{\mathbf{V}}^\top}.$$

Unfortunately, it may be the case that $\bar{\mathbf{V}}\bar{\mathbf{V}}^\top \neq \mathbf{I}_n$, while orthogonality is crucial in order to easily calculate the inverse of Σ_θ . An additional step is required to obtain an orthogonal version of the Nyström decomposition, as studied by [Fowlkes et al. \(2001\)](#). Let $\mathbf{K} = \mathbf{A} + \mathbf{A}^{-\frac{1}{2}}\mathbf{B}^\top\mathbf{B}\mathbf{A}^{-\frac{1}{2}}$, where $\mathbf{A}^{-\frac{1}{2}} = \mathbf{V}_m\mathbf{U}_m^{-\frac{1}{2}}\mathbf{V}_m$, and obtain the eigendecomposition of this $m \times m$ matrix $\mathbf{K} = \mathbf{R}\hat{\mathbf{U}}\mathbf{R}^\top$. Defining

$$\hat{\mathbf{V}} = \begin{pmatrix} \mathbf{A} \\ \mathbf{B}^\top \end{pmatrix} \mathbf{A}^{-\frac{1}{2}}\mathbf{R}\hat{\mathbf{U}}^{-\frac{1}{2}} \in \mathbb{R}^n \times \mathbb{R}^m,$$

then we have that $\mathbf{H}_\eta \approx \hat{\mathbf{V}}\hat{\mathbf{U}}\hat{\mathbf{V}}^\top$ such that $\hat{\mathbf{V}}\hat{\mathbf{V}}^\top = \mathbf{I}_n$. Estimating I-prior models with the Nyström method including the orthogonalisation step takes roughly $O(nm^2)$ time and $O(nm)$ storage.

The issue of selecting the subset \mathcal{Q} remains. The simplest method, and that which is implemented in the **iprior** package, would be to uniformly sample a subset of size q from the n points. Although this works well in practice, the quality of approximation might suffer if the points do not sufficiently represent the training set. In this light, greedy approximations have been suggested to select the q points, so as to reduce some error criterion relating to the quality of approximation. For a brief review of more sophisticated methods of selecting \mathcal{Q} , see [Rasmussen and Williams \(2006, §8.1, pp. 173–174\)](#).

4.3.2 Front-loading kernel matrices for the EM algorithm

The evaluation of the Q function in (4.14) is $O(n^3)$, because a change in the values of θ requires evaluating $\Sigma_\theta = \psi\mathbf{H}_\eta^2 + \psi^{-1}\mathbf{I}_n$, for which squaring \mathbf{H}_η takes the bulk of the computational time. This is disadvantageous because, a Newton or quasi-Newton algorithm used for the M-step would require multiple evaluations of Q in order to complete an EM update.

In this section, we describe an efficient method of evaluating Q if the I-prior model only involves estimating the RKHS scale parameters and the error precision under assumptions A1–A3. The premise is this: squaring an ANOVA kernel matrix can be made more efficient because it is a linear combination of several other kernel matrices, which can be pre-calculated and stored for multiple use throughout the EM algorithm. We now describe the procedure in detail.

3. Attempt to prove this.

sec:efficientEM1

Corresponding to p building block RKHSs $\mathcal{F}_1, \dots, \mathcal{F}_p$ of functions over $\mathcal{X}_1, \dots, \mathcal{X}_p$, there are p scale parameters $\lambda_1, \dots, \lambda_p$ and reproducing kernels h_1, \dots, h_p . Assume that only the scale parameters are to be estimated, and the rest of the kernel parameters (Hurst coefficient, lengthscale, or offset) are fixed. Write $\theta = \{\lambda_1, \dots, \lambda_p, \psi\}$. The most common modelling scenarios that will be encountered are listed below:

1. **Single scale parameter.** With $p = 1$, $f \in \mathcal{F} \equiv \lambda_1 \mathcal{F}_1$ of functions over a set \mathcal{X} . \mathcal{F} may be any of the building block RKHSs. Note that \mathcal{X}_1 itself may be more than one-dimensional. The kernel over $\mathcal{X}_1 \times \mathcal{X}_1$ is therefore

$$h_\lambda = \lambda_1 h_1.$$

2. **Multiple scale parameters.** Here, \mathcal{F} is a RKKS of functions $f : \mathcal{X}_1 \times \dots \times \mathcal{X}_p \rightarrow \mathbb{R}$, and thus $\mathcal{F} \equiv \lambda_1 \mathcal{F}_1 \oplus \dots \oplus \lambda_p \mathcal{F}_p$, where each \mathcal{F}_k is one of the building block RKHSs. The kernel is

$$h_\lambda = \lambda_1 h_1 + \dots + \lambda_p h_p.$$

3. **Multiple scale parameters with level-2 interactions.** This occurs commonly with multilevel and longitudinal models. Suppose that \mathcal{X}_1 is the set of ‘levels’ and there are $p - 1$ covariate sets \mathcal{X}_k , $k = 2, \dots, p$. The function space \mathcal{F} is a special case of the ANOVA RKKS containing only main and two-way interaction effects, and its kernel is

$$h_\lambda = \sum_{j=1}^p \lambda_j h_j + \sum_{j < k} \lambda_j \lambda_k h_j h_k,$$

where \mathcal{F}_1 is the Pearson RKHS, and the remaining are any of the building block RKHSs.

4. **Polynomial RKKS.** When using the polynomial RKKS of degree d to incite a polynomial relationship of the covariate set \mathcal{X}_1 on the function $f \in \mathcal{F}$ (excluding an intercept), then the kernel of \mathcal{F} is

$$h_\lambda = \sum_{k=1}^d b_k \lambda_1^k h_1^k.$$

where $b_k = \frac{d!}{k!(d-k)!}$, $k = 1, \dots, d$ are constants.

Of course, many other models are possible, such as the ANOVA RKKS with all p levels of interactions. What we realise is that any of these scenarios are simply a sum-product

of a manipulation of the set of scale parameters $\lambda = \{\lambda_1, \dots, \lambda_p\}$ and the set of kernel functions $h = \{h_1, \dots, h_p\}$.

Let us be more concrete about what we mean by ‘manipulation’ of the sets λ and h . Define an ‘instruction operator’ which expands out both sets identically as required by the modelling scenario. Computationally speaking, this instruction could be carried out through an instructive list \mathcal{Q} containing the indices to multiply out. For the four scenarios above, the list \mathcal{Q} are as follows:

1. $\mathcal{Q} = \{\{1\}\}$.
2. $\mathcal{Q} = \{\{1\}, \dots, \{p\}\}$.
3. $\mathcal{Q} = \{\{1\}, \dots, \{p\}, \{1, 2\}, \dots, \{p-1, p\}\}$.
4. $\mathcal{Q} = \{\{1\}, \{1, 1\}, \dots, \overbrace{\{1, \dots, 1\}}^d\}$.

For the polynomial RKKS in the fourth example, one must also multiply the constants b_k to the λ ’s as appropriate. Let q be the cardinality of the set \mathcal{Q} , which is the number of summands required to construct the kernel for \mathcal{F} . Denote the instructed sets as $\xi = \{\xi_1, \dots, \xi_q\}$ for λ and $a = \{a_1, \dots, a_q\}$ for h . We can write the kernel h_λ as a linear combination of ξ and a ,

$$h_\lambda = \xi_1 a_1 + \dots + \xi_q a_q.$$

The reason this is important is because changes in λ for h_λ only changes the ξ_k ’s, but not the a_k ’s. This allows us to compute and store all of the required $n \times n$ kernel matrices $\mathbf{A}_1, \dots, \mathbf{A}_q$ by application of the instruction set \mathcal{Q} on h , evaluated at all pairs of data points $(x_i, x_j) \in \mathcal{X} \times \mathcal{X}$. This process of initialisation need only be done once prior to commencing the EM algorithm—a step we refer to as ‘kernel loading’.

Notice that

$$\begin{aligned} \text{tr}(\Sigma_\theta \tilde{\mathbf{W}}^{(t)}) &= \text{tr}((\psi \mathbf{H}_\eta^2 + \psi^{-1} \mathbf{I}_n) \tilde{\mathbf{W}}^{(t)}) \\ &= \psi \text{tr}(\mathbf{H}_\eta^2 \tilde{\mathbf{W}}^{(t)}) + \psi^{-1} \text{tr} \tilde{\mathbf{W}}^{(t)} \\ &= \psi \text{tr} \left(\sum_{j,k=1}^q \xi_j \xi_k (\mathbf{A}_j \mathbf{A}_k + (\mathbf{A}_j \mathbf{A}_k)^\top) \tilde{\mathbf{W}}^{(t)} \right) + \psi^{-1} \text{tr} \tilde{\mathbf{W}}^{(t)} \\ &= 2\psi \sum_{j,k=1}^q \xi_j \xi_k \text{tr}(\mathbf{A}_j \mathbf{A}_k \tilde{\mathbf{W}}^{(t)}) + \psi^{-1} \text{tr} \tilde{\mathbf{W}}^{(t)}. \end{aligned}$$

Provided that we have the matrices $\mathbf{A}_{jk} = \mathbf{A}_j \mathbf{A}_k$, $j, k = 1, \dots, q$ in addition to $\mathbf{A}_1, \dots, \mathbf{A}_q$ pre-calculated and stored, then evaluating $\text{tr}(\mathbf{A}_{jk} \tilde{\mathbf{W}}^{(t)}) = \text{vec}(\mathbf{A}_{jk})^\top \text{vec}(\tilde{\mathbf{W}}^{(t)})$ is $O(n^2)$, although this only need to be done once per EM iteration. Thus, with the kernels loaded, the overall time complexity to evaluate Q is $O(n^2)$ at the beginning of each iteration, but roughly linear in ξ thereafter.

As a remark, we have achieved efficiency at the expense of storage and a potentially long initialisation phase of kernel loading. In the **iprior** package, kernel loading is performed using the `kernL()` command. The storing of the kernel matrices can be very expensive, especially if the sample size is very large; Figure 4.3 shows the storage cost of front-loading the kernel matrices for varying number of ANOVA components $p = 1, \dots, 5$ and sample sizes. On the bright side, once the kernel matrices are stored in hard memory, the **iprior** package allows them to be reused again and again. A practical situation where this might be useful is when we would like to repeat the EM at various initial values. Although front-loading of kernel matrices increase storage requirements, this is manageable in practice in modern computer systems for sample sizes of $n \leq 5,000$, and there is a clear advantage of doing so.

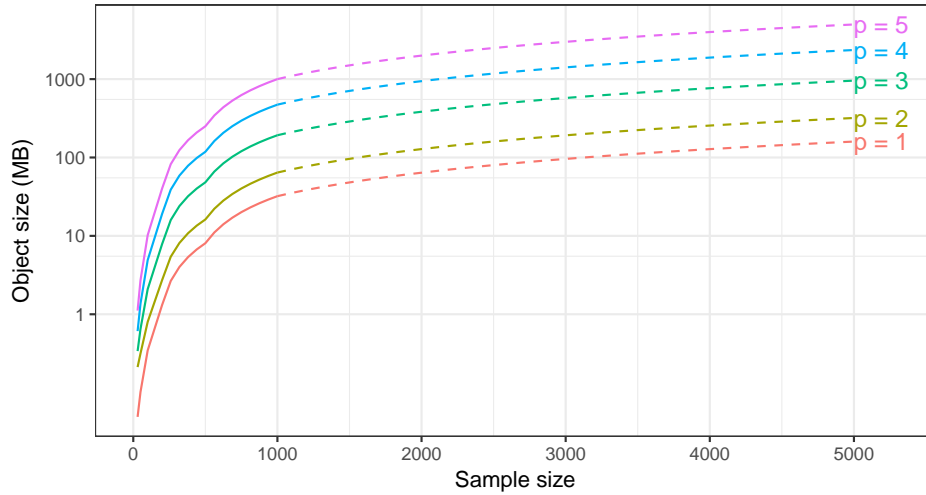


Figure 4.3: Storage cost of front-loading the kernel matrices for varying number of ANOVA components $p = 1, \dots, 5$ and sample sizes. Solid lines indicate actual values, while dotted lines represent (linear) predictions. Storage requirements increases exponentially, since for p ANOVA components, there are 2^{p+1} kernel matrices to store in memory.

fig:ipriors
storage

sec:expfamE
M

4.3.3 The exponential family EM algorithm

In the original EM paper by [Dempster et al. \(1977\)](#), the EM algorithm was demonstrated to be easily administered to complete data likelihoods belonging to the exponential family for which the maximum likelihood estimates are easily computed. If this is the case, then the M-step simply involves replacing the unknown sufficient statistics in the ML estimates with their *conditional expectations*. Certain I-prior models admit this property, namely regression functions belonging to the full or limited ANOVA RKKS. For such models, we can reduce the EM algorithm to a sequential updating scheme of the latent variables (missing data) and parameters, bypassing the need for a gradient-based optimisation in the M-step. We describe the implementation of this exponential family EM below.

Assume [A1–A3](#) applies, and that only the error precision ψ and the RKHS scale parameters $\lambda_1, \dots, \lambda_p$ need to be estimated, i.e. all other kernel parameters are fixed—a similar situation was described in the previous subsection. For the full ANOVA RKKS, the kernel can be written in the form

$$\begin{aligned}
 h_\lambda &= \sum_{i=1}^p \lambda_i h_i + \underbrace{\sum_{i < j} \lambda_i \lambda_j h_i h_j + \dots + \prod_{i=1}^p \lambda_i h_i}_{\text{terms of } \lambda_k} \\
 &= \lambda_k \left(\underbrace{h_k + \sum_i \lambda_i h_i h_k + \dots + h_k \prod_{i \neq k} \lambda_i h_i}_{\text{terms of } \lambda_k} \right) + \underbrace{\sum_{i \neq k} \lambda_i h_i + \sum_{i, j \neq k} \lambda_i \lambda_j h_i h_j + \dots + 0}_{\text{no } \lambda_k \text{ here}} \\
 &= \lambda_k r_k + s_k
 \end{aligned}$$

where r_k and s_k are both functions over $\mathcal{X} \times \mathcal{X}$, defined respectively as the terms of the ANOVA kernel involving λ_k , and the terms not involving λ_k . The reason for splitting h_λ like this will become apparently momentarily.

Programmatically, this looks complicated to implement in software, but in fact it is not. Consider again the instruction list \mathcal{Q} for the ANOVA RKKS (Example 3, [Section 4.3.2](#)). We can split this list into two: \mathcal{R}_k as those elements of \mathcal{Q} which involve the index k , and \mathcal{S}_k as those elements of \mathcal{Q} which do not involve the index k . Let ζ_k, e_k be the sets of λ and h after applying the instructions of \mathcal{R}_k , and let ξ_k and a_k be the sets

of λ and h after application of the instruction list \mathcal{S}_k . Now, we have

$$r_k = \frac{1}{\lambda_k} \sum_{l=1}^{|\mathcal{R}_k|} \zeta_{lk} e_{lk} \quad \text{and} \quad s_k = \sum_{l=1}^{|\mathcal{S}_k|} \xi_{lk} a_{lk},$$

as real-valued functions defined over $\mathcal{X} \times \mathcal{X}$. Defining \mathbf{R}_k and \mathbf{S}_k as the kernel matrices with (i, j) entries $r_k(x_i, x_j)$ and $s_k(x_i, x_j)$ respectively, for $i, j = 1, \dots, n$, we have that

$$\mathbf{H}_\eta^2 = \lambda_k^2 \mathbf{R}_k^2 + \lambda_k \overbrace{(\mathbf{R}_k \mathbf{S}_k + (\mathbf{R}_k \mathbf{S}_k)^\top)}^{\mathbf{U}_k} + \mathbf{S}_k^2.$$

Consider now the full data log-likelihood for λ_k , $k = 1, \dots, p$, conditionally dependent on the rest of the unknown parameters $\lambda_{-k} = \{\lambda_1, \dots, \lambda_p\} \setminus \{\lambda_k\}$ and ψ :

$$\begin{aligned} L(\lambda_k | \mathbf{y}, \mathbf{w}, \lambda_{-k}, \psi) &= \text{const.} - \frac{1}{2} \text{tr} \left((\psi \mathbf{H}_\eta^2 + \psi^{-1} \mathbf{I}_n) \mathbf{w} \mathbf{w}^\top \right) + \psi \tilde{\mathbf{y}}^\top \mathbf{H}_\eta \mathbf{w} \\ &= \text{const.} - \lambda_k^2 \frac{\psi}{2} \text{tr}(\mathbf{R}_k^2 \mathbf{w} \mathbf{w}^\top) + \lambda_k \left(\psi \tilde{\mathbf{y}}^\top \mathbf{R}_k \mathbf{w} - \frac{\psi}{2} \text{tr}(\mathbf{U}_k \mathbf{w} \mathbf{w}^\top) \right). \end{aligned} \tag{4.19}$$

{eq:loglik1
ambdak}

Notice that the above likelihood is an exponential family distribution with the natural parameterisation $\beta = (-\lambda_k^2, \lambda_k)$ and sufficient statistics T_1 and T_2 defined by

$$T_1 = \frac{\psi}{2} \text{tr}(\mathbf{R}_k^2 \mathbf{w} \mathbf{w}^\top) \quad \text{and} \quad T_2 = \psi \tilde{\mathbf{y}}^\top \mathbf{R}_k \mathbf{w} - \frac{\psi}{2} \text{tr}(\mathbf{U}_k^2 \mathbf{w} \mathbf{w}^\top).$$

This likelihood is maximised at $\hat{\lambda}_k = T_2/2T_1$, but of course, the variables w_1, \dots, w_n are never observed. As per the exponential family EM routine, replace occurrences of \mathbf{w} and $\mathbf{w} \mathbf{w}^\top$ with their respective conditional expectations, i.e. $\mathbf{w} \mapsto \mathbb{E}[\mathbf{w} | \mathbf{y}] = \tilde{\mathbf{w}}$ and $\mathbf{w} \mathbf{w}^\top \mapsto \mathbb{E}[\mathbf{w} \mathbf{w}^\top | \mathbf{y}] = \tilde{\mathbf{V}}_w + \tilde{\mathbf{w}} \tilde{\mathbf{w}}^\top$ as defined in (4.10). That the λ_k 's have closed-form expressions, together with the closed-form expression for ψ in (4.17), greatly simplifies the EM algorithm. At the M-step, one simply updates the parameters in turn, and as such, there is no maximisation per se.

The exponential family EM algorithm for ANOVA-type I-prior models is summarised in Algorithm 1. It requires $O(n^3)$ computational time at each step, which is spent on computing the matrix inverse in the E-step. The M-step takes at most $O(n^2)$ time to compute. Algorithm 1 also requires front-loading of the kernel matrices, which increases storage requirements. As a remark, it is not necessary that h_λ is the full ANOVA RKKS;

any of the examples 1–3 in [Section 4.3.2](#) can be estimated using this method, since they are seen as special cases of the ANOVA decomposition.

Algorithm 1 Exponential family EM for ANOVA-type I-prior models

```

1: procedure INITIALISATION
2:   Initialise  $\lambda_1^{(0)}, \dots, \lambda_p^{(0)}, \psi^{(0)}$ 
3:   Compute and store matrices as per  $\mathcal{R}_k$  and  $\mathcal{S}_k$ .
4:    $t \leftarrow 0$ 
5: end procedure

6: while not converged do
7:   procedure E-STEP
8:      $\tilde{\mathbf{w}} \leftarrow \psi^{(t)} \mathbf{H}_{\eta^{(t)}} (\psi^{(t)} \mathbf{H}_{\eta^{(t)}}^2 + \psi^{-(t)} \mathbf{I}_n)^{-1} \tilde{\mathbf{y}}$ 
9:      $\tilde{\mathbf{W}} \leftarrow (\psi^{(t)} \mathbf{H}_{\eta^{(t)}}^2 + \psi^{-(t)} \mathbf{I}_n)^{-1} + \tilde{\mathbf{w}} \tilde{\mathbf{w}}^\top$ 
10:  end procedure

11:  procedure M-STEP
12:    for  $k = 1, \dots, p$  do
13:       $T_{1k} \leftarrow \frac{1}{2} \text{tr}(\mathbf{R}_k^2 \tilde{\mathbf{W}})$ 
14:       $T_{2k} \leftarrow \tilde{\mathbf{y}}^\top \mathbf{R}_k \tilde{\mathbf{w}} - \frac{1}{2} \text{tr}(\mathbf{U}_k^2 \tilde{\mathbf{W}}^\top)$ 
15:       $\lambda_k^{(t+1)} \leftarrow T_{2k} / 2T_{1k}$ 
16:    end for
17:     $T_3 \leftarrow \tilde{\mathbf{y}}^\top \tilde{\mathbf{y}} + \text{tr}(\mathbf{H}_{\eta^{(t)}}^2 \tilde{\mathbf{W}}^{(t)}) - 2\tilde{\mathbf{y}}^\top \mathbf{H}_{\eta^{(t)}} \tilde{\mathbf{w}}^{(t)}$ 
18:     $\psi^{(t+1)} \leftarrow \text{tr} \tilde{\mathbf{W}}^{(t)} / T_3$ 
19:  end procedure
20:   $t \leftarrow t + 1$ 
21: end while

```

Remark 4.5. Another compelling reason to use [Algorithm 1](#) is conjugacy of the exponential family of distributions. Realise that $\lambda_k | (\mathbf{y}, \mathbf{w}, \lambda_{-k}, \psi)$ is in fact normally distributed, with mean and variance given by $T_2/2T_1$ and $1/2T_1$ respectively. If we were so compelled to assign a normal prior on each of the λ_k 's, then the conditionally dependent log-likelihood of λ_k , $L(\lambda_k | \mathbf{y}, \mathbf{w}, \lambda_{-k}, \psi)$, would have a normal prior log-density involving λ_k added on. Importantly, viewed as a posterior log-density for λ_k , the λ_k is normally distributed. The exponential family EM is thus easily modified to compute maximum a posteriori (MAP) estimates (or penalised ML estimates) of the scale parameters. With diffuse priors on λ_k , MAP estimates are in fact ML estimates.

Remark 4.6. The restriction to ANOVA RKKSs is due to the fact that as soon as higher degrees of the λ_k 's come into play, e.g. using the polynomial kernel, then the ML

alg:EM2

estimates for the λ_k 's involve solving a polynomial of degree $2d - 1$ for FOC equations. Although this is not in itself hard to do, the elegance of the algorithm, especially viewed as having the normal conjugacy property for the λ_k 's, is lost.

4.4 Post-estimation

One of the perks of a (semi-)Bayesian approach to regression modelling is that we are able to use Bayesian post-estimation machinery involving the relevant posterior distributions. With the normal I-prior model, there is the added benefit that posterior distributions are easily obtained in closed form. We describe post-estimation procedures such as prediction of a new data point, inference surrounding the prediction, and model comparison. The plots that are shown in this subsection is a continuation of the example from [Section 4.2.5](#).

Recall that for the I-prior model [\(4.9\)](#), the regression function $f(x) = \sum_{i=1}^n h_{\hat{\eta}}(x, x_i) \tilde{w}_i$ has the posterior Gaussian distribution specified by the multivariate-normal mean and variance of the \tilde{w}_i 's given in [\(4.10\)](#). Denote by $\mathbf{h}_{\hat{\eta}}(x)$ the n -vector with entries equal to $h_{\hat{\eta}}(x, x_i)$. Precisely, the posterior density for the regression function is

$$f(x)|\mathbf{y} \sim \mathcal{N}\left(\mathbf{h}_{\hat{\eta}}(x)\hat{\mathbf{w}}, \mathbf{h}_{\hat{\eta}}(x)^\top (\mathbf{H}_{\hat{\eta}}\hat{\mathbf{\Psi}}\mathbf{H}_{\hat{\eta}} + \hat{\mathbf{\Psi}}^{-1})^{-1} \mathbf{h}_{\hat{\eta}}(x)\right) \quad (4.20)$$

for any x in the domain of the regression function. Here, the hats on the parameters indicate the use of the optimised model parameters, i.e. the ML or MAP estimates.

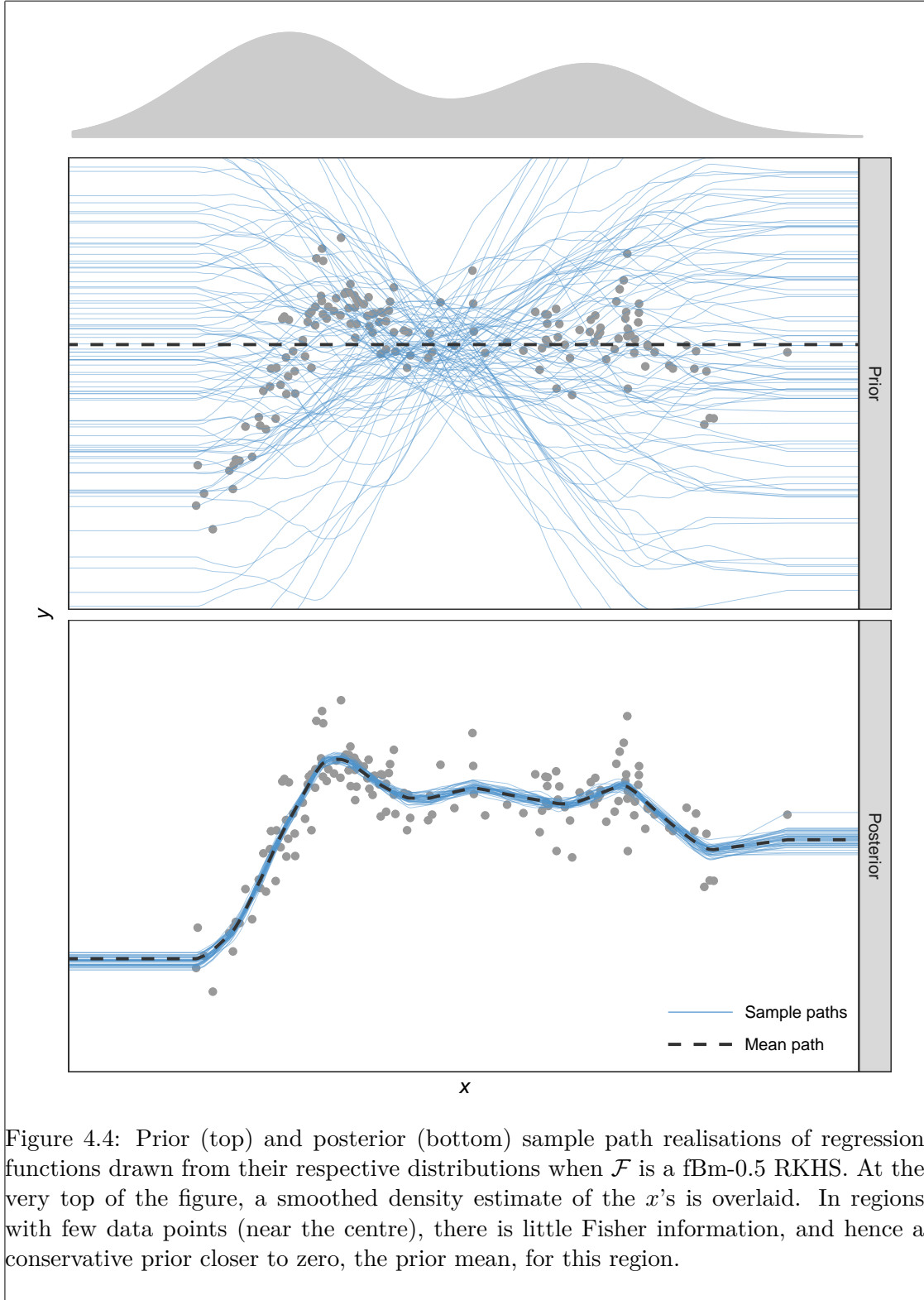
Prediction of a new data point is now described. A priori, assume that $y_{\text{new}} = \hat{\alpha} + f(x_{\text{new}}) + \epsilon_{\text{new}}$, where $\epsilon_{\text{new}} \sim \mathcal{N}(0, \psi_{\text{new}}^{-1})$, and $f \sim \text{I-prior}$. Denote the covariance between ϵ_{new} and $\boldsymbol{\epsilon} = (\epsilon_1, \dots, \epsilon_n)^\top$ by $\boldsymbol{\sigma}_{\text{new}}^\top \in \mathbb{R}^n$. Under an iid model (assumption [A3](#)), then $\psi_{\text{new}} = \psi = \text{Var } \epsilon_i$ for any $i \in \{1, \dots, n\}$, and $\boldsymbol{\sigma}_{\text{new}}^\top = \mathbf{0}$, but otherwise, these extra parameters need to be dealt with somehow, either by specifying them a priori or estimating them again, which seems excessive. In any case, using a linearity argument, the posterior distribution for y_{new} is normal, with mean and variance given by

$$\mathbb{E}[y_{\text{new}}|\mathbf{y}] = \hat{\alpha} + \mathbb{E}[f(x_{\text{new}})|\mathbf{y}] + \text{correction term} \quad (4.21)$$

and

$$\text{Var}[y_{\text{new}}|\mathbf{y}] = \text{Var}[f(x_{\text{new}})|\mathbf{y}] + \psi_{\text{new}}^{-1} + \text{correction term.} \quad (4.22)$$

sec:ipriorp
ostest



A derivation is presented in [Appendix G.2](#). Note, that the mean and variance correction term vanishes under an iid assumption [A3](#). The posterior distribution for y_{new} can be used in several ways. Among them, is to construct a $100(1 - \alpha)\%$ credibility interval for the (mean) predicted value y_{new} using

$$\mathbb{E}[y_{\text{new}}|\mathbf{y}] \pm \Phi^{-1}(1 - \alpha/2) \text{Var}[y_{\text{new}}|\mathbf{y}]^{\frac{1}{2}},$$

where $\Phi(\cdot)$ is the standard normal cumulative distribution function. One could also perform a posterior predictive density check of the data \mathbf{y} , by repeatedly sampling n points from its posterior distribution. This provides a visual check of whether there are any systematic deviances between what the model predicts, and what is observed from the data.

Lastly, we discuss model comparison. Recall that the marginal distribution for \mathbf{y} after integrating out the I-prior for f in model [\(4.9\)](#) is normal. Suppose that we are interested in comparing two candidate models M_0 and M_1 , each with parameter sets θ_0 and θ_1 . Commonly, we would like to test whether or not particular terms in the ANOVA RKKS are significant contributors in explaining the relationship between the responses and predictors. A log-likelihood comparison is possible using an asymptotic chi-squared distribution, with degrees of freedom equal to the difference between the number of parameters in M_1 and M_0 . This is assuming model M_0 is nested within M_1 , which is the case for ANOVA-type constructions. Note that if two models have the same number of parameters, then the model with the higher likelihood is preferred.

Remark 4.7. This method of comparing marginal likelihoods can be seen as Bayesian model selection using *empirical Bayes factors*, where the Bayes factor of comparing model M_1 against model M_0 is defined as

$$\text{BF}(M_1, M_0) = \frac{\int p(\mathbf{y}|\hat{\theta}_1, \mathbf{f})p(\mathbf{f}) \, d\mathbf{f}}{\int p(\mathbf{y}|\hat{\theta}_0, \mathbf{f})p(\mathbf{f}) \, d\mathbf{f}}.$$

Bayes factor values of greater than one indicate more support for model M_1 over M_0 . The term ‘empirical’ stems from the fact that the parameters are estimated via an empirical Bayes approach (maximum marginal likelihood), as opposed to assuming prior distributions on them and integrating them out.

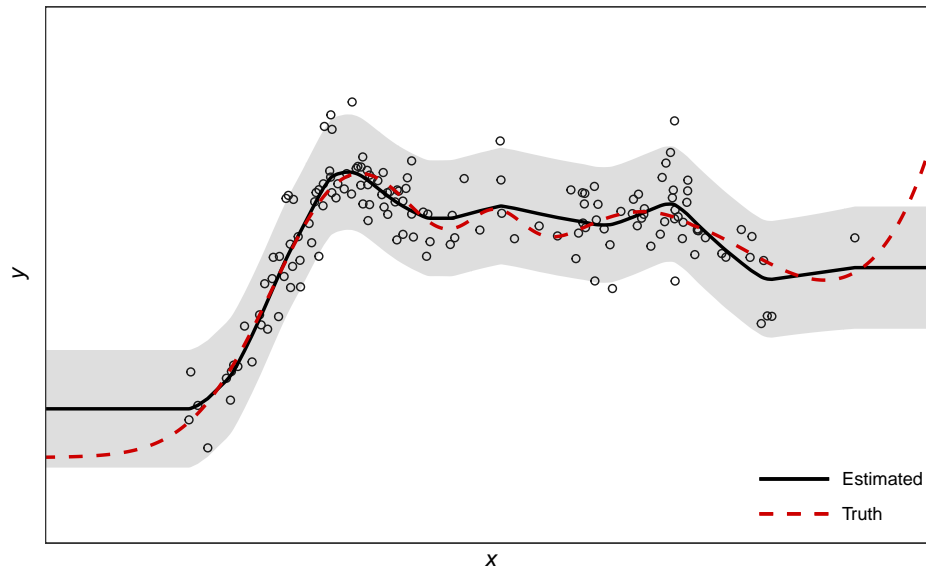


Figure 4.5: The estimated regression line (solid black) is the posterior mean estimate of the regression function (shifted by the intercept), which also gives the posterior mean estimate for the responses y . The shaded region is the 95% credibility interval for predictions. The true regression line (dashed red) is shown for comparison.

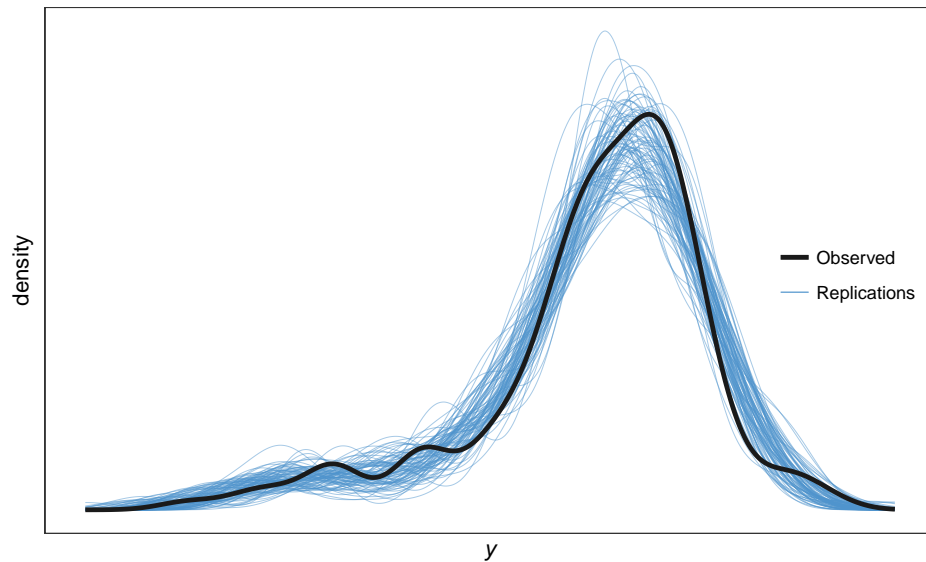


Figure 4.6: Posterior predictive density checks of the responses: repeated sampling from the posterior density of the y_i 's and plotting their densities allows us to compare model predictions against observed samples.

sec:ipriore
xamples

4.5 Examples

We demonstrate I-prior modelling on a toy data set to illustrate the Nyström method, as well as three other real-data examples. All of the analyses were conducted in R, and I-prior model estimation was done using the **iprior** package. In all of these examples, [A1–A3](#) were assumed.

4.5.1 Using the Nyström method

We investigate the use of the Nyström method of approximating the kernel matrix in estimating I-prior models. Let us revisit the data set generated by [\(4.18\)](#) described in [Section 4.2.5](#). The features of this regression function are two large bumps at the centres of the mixed Gaussian PDFs, and also a small bump right after $x > 4.5$ caused by the additional exponential function. The true regression function tends to positive infinity as x increases, and to zero as x decreases. Samples of (x_i, y_i) , $i = 1, \dots, 2000$ have been generated by the built-in `gen_smooth()` function, of which the first few lines of the data are shown below.

```
R> dat <- gen_smooth(n = 2000, xlim = c(-1, 5.5), seed = 1)
R> head(dat)

##           y           X
## 1  0.6803514 -2.608953
## 2  3.6747031 -2.554039
## 3 -1.1563508 -2.381275
## 4  2.2657657 -2.280259
## 5  2.5398243 -2.214122
## 6  1.2929592 -2.170532
```

One could fit the regression model using all available data points, with an I-prior from the fBm-0.5 RKHS of functions as follows (note that the `silent` option is used to suppress the output from the `iprior()` function):

```
R> (mod.full <- iprior(y ~ X, dat, kernel = "fbm",
+                      control = list(silent = TRUE)))

## Log-likelihood value: -4355.075
##
```

```
## lambda      psi
## 2.30244 0.23306
```

To implement the Nyström method, the option `nystrom = 50` was added to the above function call, which uses 50 randomly selected data points for the Nyström approximation.

```
R> (mod.nys <- iprior(y ~ X, dat, kernel = "fbm", nystrom = 50,
+                    control = list(silent = TRUE)))
```

```
## Log-likelihood value: -1945.33
##
## lambda      psi
## 1.64833 0.13538
```

The hyperparameters estimated for both models are slightly different. The log-likelihood is also different, but this is attributed to information loss due to the approximation procedure. Nevertheless, we see from [Figure 4.7](#) that the estimated regression functions are quite similar in both the full model and the approximated model. The main difference is that the the Nyström method was not able to extrapolate the right hand side of the plot well, because it turns out that there were no data points used from this region. This can certainly be improved by using a more intelligent sampling scheme. The full model took a little over 12 minutes to converge, while the Nyström method took seconds without compromising too much on root mean squared error of predictions. Storage savings is significantly higher with the Nyström method as well.

```
R> get_time(mod.full); get_size(mod.full, "MB"); get_prederror(mod.full)

## 12.10819 mins
## 128.2 MB
## Training RMSE
##      2.054232

R> get_time(mod.nys); get_size(mod.nys); get_prederror(mod.nys)

## 1.287808 secs
## 982.2 kB
## Training RMSE
##      2.171928
```

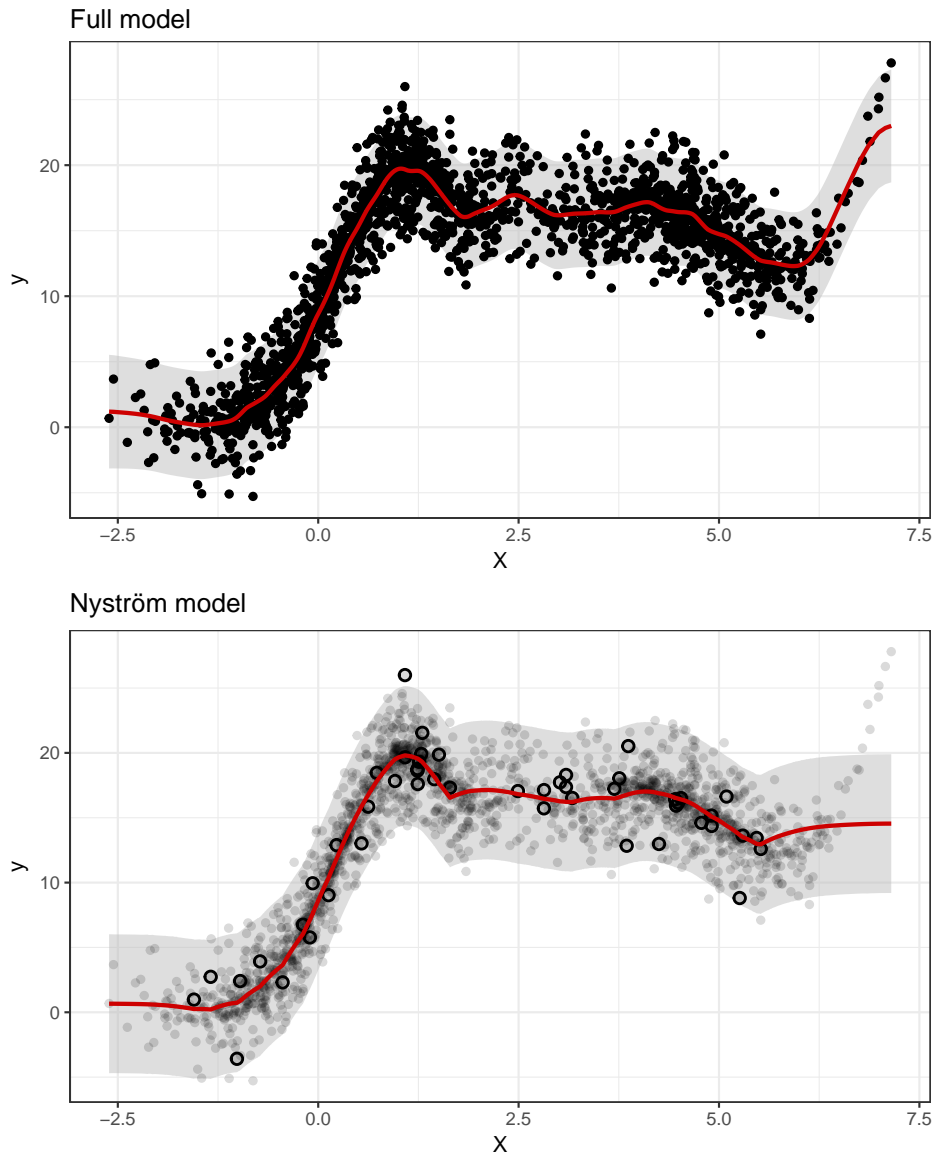


Figure 4.7: Plot of predicted regression function for the full model (top) and the Nyström approximated method (bottom). For the Nyström plot, the data points that were active are shown by circles with bold outlines.

fig:nystrom
.plot

4.5.2 Random effects models

In this section, a comparison between a standard random effects model and the I-prior approach for estimating varying intercept and slopes model is illustrated. The example concerns control data³ from several runs of radioimmunoassays (RIA) for the protein insulin-like growth factor (IGF-I) (explained in further detail in [Davidian and Giltinan, 1995, §3.2.1](#)). RIA is an in vitro assay technique which is used to measure concentration of antigens—in our case, the IGF-I proteins. When an RIA is run, control samples at known concentrations obtained from a particular lot are included for the purpose of assay quality control. It is expected that the concentration of the control material remains stable as the machine is used, up to a maximum of about 50 days, at which point control samples from a new batch is used to avoid degradation in assay performance.

```
R> data(IGF, package = "nlme")
R> head(IGF)

## Grouped Data: conc ~ age | Lot
##   Lot age conc
## 1    1   7 4.90
## 2    1   7 5.68
## 3    1   8 5.32
## 4    1   8 5.50
## 5    1  13 4.94
## 6    1  13 5.19
```

The data consists of IGF-I concentrations (`conc`) from control samples from 10 different lots measured at differing `ages` of the lot. The data were collected with the aim of identifying possible trends in control values `conc` with `age`, ultimately investigating whether or not the usage protocol of maximum sample age of 50 days is justified. [J. C. Pinheiro and Bates \(2000\)](#) remarks that this is not considered a longitudinal problem because different samples were used at each measurement.

We shall model the IGF data set using the I-prior methodology using the ANOVA-decomposed regression function

$$f(\text{age}, \text{Lot}) = f_1(\text{age}) + f_2(\text{Lot}) + f_{12}(\text{age}, \text{Lot})$$

³This data is available in the R package `nlme` ([J. Pinheiro et al., 2017](#)).

where f_1 lies in the linear RKHS \mathcal{F}_1 , f_2 in the Pearson RKHS \mathcal{F}_2 and f_{12} in the tensor product space $\mathcal{F}_{12} = \mathcal{F}_1 \otimes \mathcal{F}_2$. The regression function f then lies in the RKHS $\mathcal{F} = \mathcal{F}_1 \oplus \mathcal{F}_2 \oplus \mathcal{F}_{12}$ with kernel equal to the sum of the kernels from each of the RKHSs. The explanation here is that the `conc` levels are assumed to be related to both `age` and `Lot`, and in particular, the contribution of `age` on `conc` varies with each individual `Lot`. This gives the intended effect of a linear mixed-effects model, which is thought to be suitable in this case, in order to account for within-lot and between-lot variability. We first fit the model using the `iprior` package, and then compare the results with the standard random effects model using the R command `lme4::lmer()`. The command to fit the I-prior model using the EM algorithm is

```
R> mod.iprior <- iprior(conc ~ age * Lot, IGF, method = "em")

## =====
## Converged after 57 iterations.

R> summary(mod.iprior)

## Call:
## iprior(formula = conc ~ age * Lot, data = IGF, method = "em")
##
## RKHS used:
## Linear (age)
## Pearson (Lot)
##
## Residuals:
##      Min. 1st Qu.  Median 3rd Qu.    Max.
## -4.4889 -0.3798 -0.0090  0.2563  4.3973
##
## Hyperparameters:
##           Estimate   S.E.      z P[|Z>z|]
## lambda[1]  0.0000 0.0002 -0.004   0.997
## lambda[2]  0.0007 0.0030  0.238   0.812
## psi        1.4576 0.1366 10.672 <2e-16 ***
## ---
## Signif. codes:  0 '***' 0.001 '**' 0.01 '*' 0.05 '.' 0.1 ' ' 1
##
## Closed-form EM algorithm. Iterations: 57/100
```

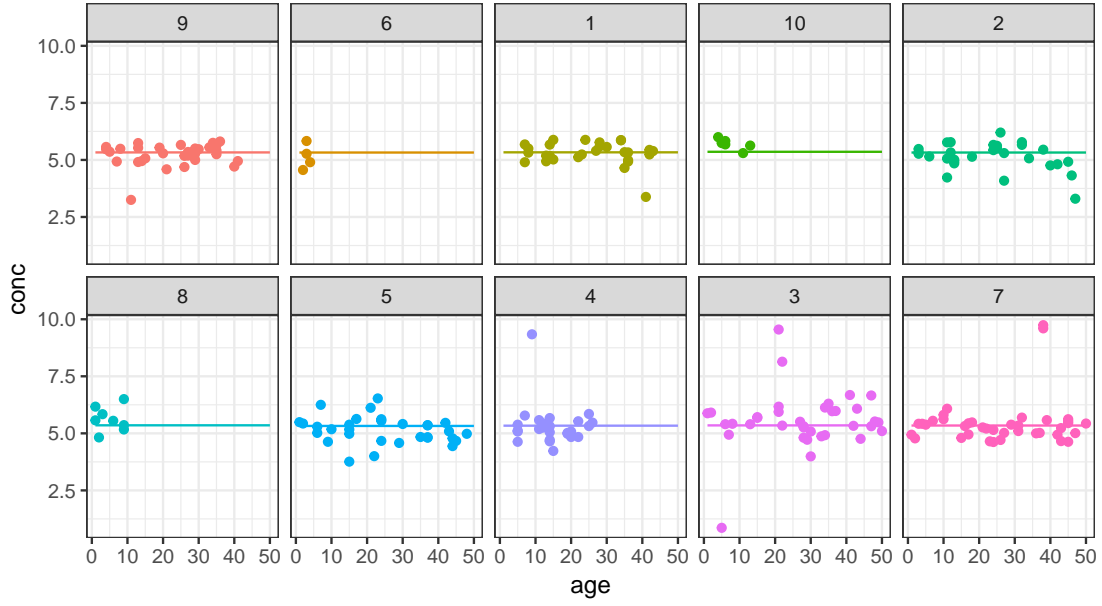


Figure 4.8: Plot of fitted regression line for the I-prior model on the IGF data set, separated into each of the 10 lots.

fig:IGF.mod
.iprior.plot

```
## Converged to within 1e-08 tolerance. Time taken: 2.882966 secs
## Log-likelihood value: -291.9033
## RMSE of prediction: 0.8273639 (Training)
```

To make inference on the covariates, we look at the scale parameters `lambda`. We see that both scale parameters for `age` and `Lot` are close to zero, and a test of significance is not able to reject the hypothesis that these parameters are indeed null. We conclude that neither `age` nor `Lot` has a linear effect on the `conc` levels. The plot of the fitted regression line in [Figure 4.8](#) does show an almost horizontal line for each `Lot`.

The standard random effects model, as explored by [Davidian and Giltinan \(1995\)](#) and [J. C. Pinheiro and Bates \(2000\)](#), is

$$\begin{aligned} \text{conc}_{ij} &= \beta_{0j} + \beta_{1j}\text{age}_{ij} + \epsilon_{ij} \\ \begin{pmatrix} \beta_{0j} \\ \beta_{1j} \end{pmatrix} &\sim N\left(\begin{pmatrix} \beta_0 \\ \beta_1 \end{pmatrix}, \begin{pmatrix} \sigma_0^2 & \sigma_{01} \\ \sigma_{01} & \sigma_1^2 \end{pmatrix}\right) \\ \epsilon_{ij} &\sim N(0, \sigma^2) \end{aligned}$$

for $i = 1, \dots, n_j$ and the index j representing the 10 Lots. Fitting this model using `lmer`, we can test for the significance of the fixed effect β_0 , for which we find that it is not (p -value = 0.616), and arrive at the same conclusion as in the I-prior model. However, we notice that the package reports a perfect negative correlation between the random effects, σ_{01} . This indicates a potential numerical issue when fitting the model—a value of exactly -1 , 0 or 1 is typically imposed by the package to force through estimation in the event of non-positive definite covariance matrices arising. We can inspect the eigenvalues of the covariance matrix for the random effects to check that they are indeed non-positive definite.

```
R> (mod.lmer <- lmer(conc ~ age + (age | Lot), IGF))

## Linear mixed model fit by REML ['lmerMod']
## Formula: conc ~ age + (age | Lot)
##      Data: IGF
## REML criterion at convergence: 594.3662
## Random effects:
##   Groups   Name      Std.Dev. Corr
##   Lot      (Intercept) 0.082507
##           age          0.008092 -1.00
## Residual                0.820628
## Number of obs: 237, groups: Lot, 10
## Fixed Effects:
## (Intercept)                age
##    5.374974        -0.002535

R> eigen(VarCorr(mod.lmer)$Lot)

## eigen() decomposition
## $values
## [1]  6.872939e-03 -1.355253e-20
##
## $vectors
##           [,1]      [,2]
## [1,] -0.99522490 -0.09760839
## [2,]  0.09760839 -0.99522490
```

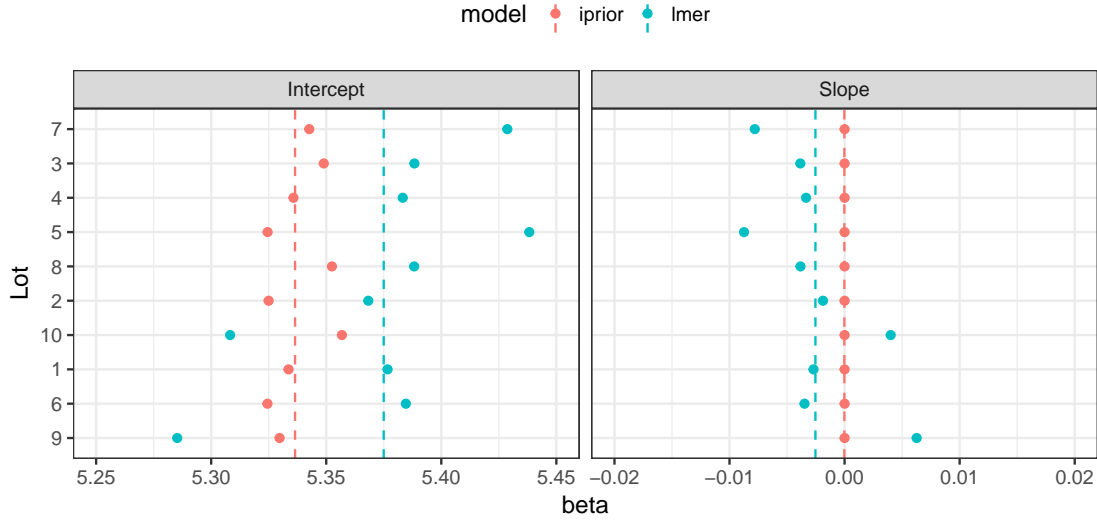



Figure 4.9: A comparison of the estimates for random intercepts and slopes (denoted as points) using the I-prior model and the standard random effects model. The dashed vertical lines indicate the fixed effect values.

fig:IGF.plo
t.beta

Degenerate covariance matrices often occur in models with a large number of random coefficients, and in cases where values of the variance components are estimated at the boundary. These are typically solved by setting restrictions which then avoids overparameterising the model. One advantage of the I-prior method for varying intercept/slopes model is that the positive-definiteness is automatically taken care of. Furthermore, I-prior models typically require less number of parameters to fit a similar varying intercept/slopes model – in the above example, the I-prior model estimated only three parameters, while the standard random effects model estimated a total of six parameters.

It is also possible to “recover” the estimates of the standard random effects model from the I-prior model, albeit in a slightly manual fashion (refer to [Section 4.1.2](#)). Denote by f^j the individual linear regression lines for each of the $j = 1, \dots, 10$ Lots. Then, each of these f^j has a slope and intercept for which we can estimate from the fitted values $\hat{f}^j(x_{ij})$, $i = 1, \dots, n_j$. This would give us the estimate of the posterior mean of the random intercepts and slopes; these would typically be obtained using empirical-Bayes methods in the case of the standard random effects model.

Furthermore, σ_0^2 and σ_1^2 gives a measure of variability of the intercepts and slopes of the different groups, and this can be calculated from the estimates of the random inter-

cepts and slopes. In the same spirit, $\rho_{01} = \sigma_{01}/(\sigma_0\sigma_1)$, which is the correlation between the random intercept and slope, can be similarly calculated. Finally, the fixed effects can be estimated from the intercept and slope of the best fit line running through the I-prior estimated `conc` values. The intuition for this is that the fixed effects are essentially the ordinary least squares (OLS) of a linear model if the groupings are disregarded. [Figure 4.9](#) illustrates the differences in the estimates for the random coefficients, while [Table 4.2](#) illustrates the differences in the estimates for the covariance matrix. Minor differences do exist, with the most noticeable one being that the slopes in the I-prior model are categorically estimated as zero, and the sign of the correlation ρ_{01} being opposite in both models. Even so, the conclusions from both models are similar.

Table 4.2: A comparison of the estimates for the covariance matrix of the random effects using the I-prior model and the standard random effects model.

Parameter	iprior	lmer
σ_0	0.012	0.083
σ_1	0.000	0.008
ρ_{01}	0.690	-1.000

4.5.3 Longitudinal data analysis

We consider a balanced longitudinal data set consisting of weights in kilograms of 60 cows, 30 of which were randomly assigned to treatment group A, and the remaining 30 to treatment group B. The animals were weighed 11 times over a 133-day period; the first 10 measurements for each animal were made at two-week intervals and the last measurement was made one week later. This experiment was reported by [Kenward \(1987\)](#), and the data set is included as part of the package `jmcm` ([J. Pan and Y. Pan, 2016](#)) in R. The variable names have been renamed for convenience.

```
R> data(cattle, package = "jmcm")
R> names(cattle) <- c("id", "time", "group", "weight")
R> cattle$id <- as.factor(cattle$id) # convert to factors
R> levels(cattle$group) <- c("Treatment A", "Treatment B")
R> str(cattle)

## 'data.frame': 660 obs. of 4 variables:
## $ id : Factor w/ 60 levels "1","2","3","4",...: 1 1 1 1 1 1 1 1 1..
```

Table 4.3: A brief description of the five models fitted using I-priors.

Model	Explanation	Formula (<code>weight ~ ...</code>)
1	Growth does not vary with treatment nor among cows	<code>time</code>
2	Growth varies among cows only	<code>id * time</code>
3	Growth varies with treatment only	<code>group * time</code>
4	Growth varies with treatment and among cows	<code>id * time + group * time</code>
5	Growth varies with treatment and among cows, with an interaction effect between treatment and cows	<code>id * group * time</code>

```
## $ time : num  0 14 28 42 56 70 84 98 112 126 ...
## $ group : Factor w/ 2 levels "Treatment A",...: 1 1 1 1 1 1 1 1 1 1 ..
## $ weight: int  233 224 245 258 271 287 287 287 290 293 ...
```

The response variable of interest are the `weight` growth curves, and the aim is to investigate whether a treatment effect is present. The usual approach to analyse a longitudinal data set such as this one is to assume that the observed growth curves are realizations of a Gaussian process. For example, [Kenward \(1987\)](#) assumed a so-called ante-dependence structure of order k , which assumes an observation depends on the previous k observations, but given these, is independent of any preceding observations.

Using the I-prior, it is not necessary to assume the growth curves were drawn randomly. Instead, it suffices to assume that they lie in an appropriate function class. For this example, we assume that the function class is the fBm RKHS, i.e., we assume a smooth effect of time on weight. The growth curves form a multidimensional (or functional) response equivalent to a “wide” format of representing repeated measures data. In our analysis using the `iprior` package, we used the “long” format and thus our (unidimensional) sample size n is equal to 60 cows \times 11 repeated measurements. We also have two covariates potentially influencing growth, namely the cow subject `id` and also treatment `group`. The regression model can then be thought of as

$$\text{weight} = \alpha + f(\text{id}, \text{group}, \text{time}) + \epsilon$$

$$\epsilon \sim N(0, \psi^{-1}).$$

We assume iid errors, and in addition to a smooth effect of `time`, we further assume a nominal effect of both cow `id` and treatment `group` using the Pearson RKHS. In the `iprior` package, factor type objects are treated with the Pearson kernel automatically, and the only `model` option we need to specify is the `kernel = "fbm"` option for the `time` variable. We have opted not to estimate the Hurst coefficient in the interest of computational time, and instead left it at the default value of 0.5. [Table 4.3](#) explains the five models we have fitted.

The simplest model fitted was one in which the growth curves do not depend on the treatment effect or individual cows. We then added treatment effect and the cow `id` as covariates, separately first and then together at once. We also assumed that both of these covariates are time-varying, and hence added also the interaction between these covariates and the `time` variable. The final model was one in which an interaction between treatment effect and individual cows was assumed, which varied over time.

All models were fitted using the `mixed` estimation method. Compared to the EM algorithm alone, we found that the combination of direct optimisation with the EM algorithm fits the model about six times faster for this data set due to slow convergence of EM algorithm. Here is the code and output for fitting the first model:

```
R> # Model 1: weight ~ f(time)
R> set.seed(456)
R> (mod1 <- iprior(weight ~ time, cattle, kernel = "fbm", method = "mixed"))

## Running 5 initial EM iterations
## =====
## Now switching to direct optimisation
## final value 1394.615062
## converged
## Log-likelihood value: -2789.231
##
## lambda      psi
## 0.83592 0.00375
```

The results of the model fit are summarised in [Table 4.4](#). We can test for a treatment effect by testing Model 4 against the alternative that Model 2 is true. The log-likelihood ratio test statistic is $D = -2(-2791.42 - (-2270.85)) = 1041.14$, which has an asymp-

Table 4.4: Summary of the five I-prior models fitted to the cow data set. Error S.D. refers to the inverse square root of the error precision, $\psi^{-1/2}$.

Model	Formula (weight ~ ...)	Log-likelihood	Error S.D.	Number of parameters
1	time	-2789.23	16.33	1
2	id * time	-2791.42	16.39	2
3	group * time	-2295.16	3.68	2
4	id * time + group * time	-2270.85	3.39	3
5	id * group * time	-2249.26	3.90	3

totic chi-squared distribution with $3 - 2 = 1$ degree of freedom. The p -value for this likelihood ratio test is less than 10^{-6} , so we conclude that Model 4 is significantly better.

We can next investigate whether the treatment effect differs among cows by comparing Model 5 against Model 4. As these models have the same number of parameters, we can simply choose the one with the higher likelihood, which is Model 5. We conclude that treatment does indeed have an effect on growth, and that the treatment effect differs among cows. A plot of the fitted regression curves onto the cow data set is shown in Figure 4.10.

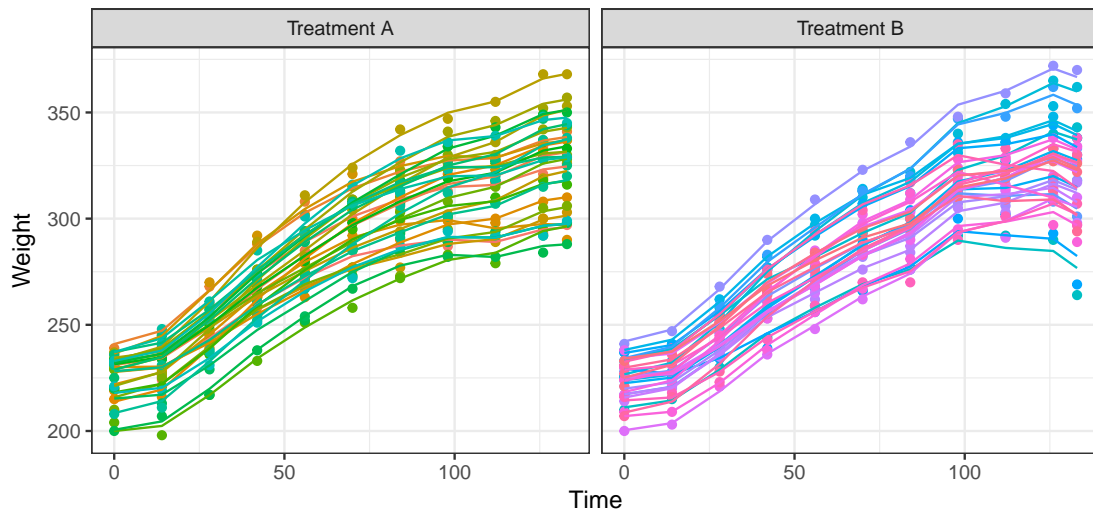


Figure 4.10: A plot of the I-prior fitted regression curves from Model 5. In this model, growth curves differ among cows and by treatment effect (with an interaction between cows and treatment effect), thus producing these 60 individual lines, one for each cow, split between their respective treatment groups (A or B).

4.5.4 Regression with a functional covariate

We illustrate the prediction of a real valued response with a functional covariate using a widely analysed data set for quality control in the food industry. The data⁴ contain samples of spectrometric curve of absorbances of 215 pieces of finely chopped meat, along with their water, fat and protein content. These data are recorded on a Tecator Infratec Food and Feed Analyzer working in the wavelength range 850–1050 nm by the Near Infrared Transmission (NIT) principle. Absorption data has not been measured continuously, but instead 100 distinct wavelengths were obtained. Figure 4.11 shows a sample of 10 such spectrometric curves.

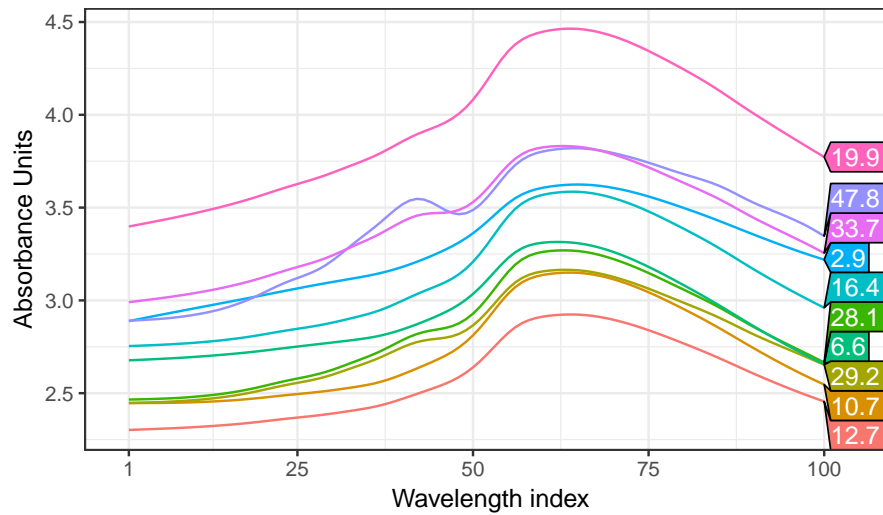


Figure 4.11: Sample of spectrometric curves used to predict fat content of meat. For each meat sample the data consists of a 100 channel spectrum of absorbances and the contents of moisture, fat (numbers shown in boxes) and protein measured in percent. The absorbance is $-\log_{10}$ of the transmittance measured by the spectrometer. The three contents, measured in percent, are determined by analytic chemistry.

fig:tecator
.data

For our analyses and many others' in the literature, the first 172 observations in the data set are used as a training sample for model fitting, and the remaining 43 observations as a test sample to evaluate the predictive performance of the fitted model. The focus here is to use the **iprior** package to fit several I-prior models to the Tecator data set, and calculate out-of-sample predictive error rates. We compare the predictive performance of I-prior models against Gaussian process regression and the many other

⁴Obtained from Tecator (see <http://lib.stat.cmu.edu/datasets/tecator> for details). We used the version made available in the dataframe **tecator** from the R package **caret** (Kuhn et al., 2017).

different methods applied on this data set. These methods include neural networks (Thodberg, 1996), kernel smoothing (Ferraty and Vieu, 2006), single and multiple index functional regression models (Chen et al., 2011), sliced inverse regression (SIR) and sliced average variance estimation (SAVE), multivariate adaptive regression splines (MARS), partial least squares (PLS), and functional additive model with and without component selection (FAM & CSEFAM). An analysis of this data set using the SIR and SAVE methods were conducted by Lian and Li (2014), while the MARS, PLS and (CSE)FAM methods were studied by Zhu et al. (2014). Table 4.5 tabulates the results of all of these methods from the various references.

Assuming a regression model as in (4.9), we would like to model the fat content y_i using the spectral curves x_i . Let $x_i(t)$ denote the absorbance for wavelength $t = 1, \dots, 100$. From Figure 4.11, it appears that the curves are smooth enough to be differentiable, and therefore it is reasonable to assume that they lie in the Sobolev-Hilbert space as discussed in Section 4.1.6. We take first differences of the 100-dimensional matrix, which leaves us with the 99-dimensional covariate saved in the object named `absorp`. The `fat` and `absorp` data have been split into `*.train` and `*.test` samples, as mentioned earlier. Our first modelling attempt is to fit a linear effect by regressing the responses `fat.train` against a single high-dimensional covariate `absorp.train` using the linear RKHS and the direct optimisation method.

```
R> # Model 1: Canonical RKHS (linear)
R> (mod1 <- iprior(y = fat.train, absorp.train))

## iter    10 value 222.653144
## final   value 222.642108
## converged
## Log-likelihood value: -445.2844
##
##      lambda      psi
## 4576.86595    0.11576
```

Our second and third model uses polynomial RKHSs of degrees two and three, which allows us to model quadratic and cubic terms of the spectral curves respectively. We also opted to estimate a suitable offset parameter, and this is called to `iprior()` with the option `est.offset = TRUE`. Each of the two models has a single scale parameter, an offset parameter, and an error precision to be estimated. The direct optimisation

method has been used, and while both models converged regularly, it was noticed that there were multiple local optima that hindered the estimation (output omitted).

```
R> # Model 2: Polynomial RKHS (quadratic)
R> mod2 <- iprior(y = fat.train, absorp.train, kernel = "poly2",
+               est.offset = TRUE)
R> # Model 3: Polynomial RKHS (cubic)
R> mod3 <- iprior(y = fat.train, absorp.train, kernel = "poly3",
+               est.offset = TRUE)
```

Next, we attempt to fit a smooth dependence of fat content on the spectrometric curves using the fBm RKHS. By default, the Hurst coefficient for the fBm RKHS is set to be 0.5. However, with the option `est.hurst = TRUE`, the Hurst coefficient is included in the estimation procedure. We fit models with both a fixed value for Hurst (at 0.5) and an estimated value for Hurst. For both of these models, we encountered numerical issues when using the direct optimisation method. The L-BFGS algorithm kept on pulling the hyperparameter towards extremely high values, which in turn made the log-likelihood value greater than the machine's largest normalised floating-point number (`.Machine$double.xmax = 1.797693e+308`). To circumvent this issue, we used the EM algorithm to estimate the fixed Hurst model, and the `mixed` method for the estimated Hurst model. For both models, the `stop.crit` was relaxed and set to `1e-3` for quicker convergence, though this did not affect the predictive abilities compared to a more stringent `stop.crit`.

```
R> # Model 4: fBm RKHS (default Hurst = 0.5)
R> (mod4 <- iprior(y = fat.train, absorp.train, kernel = "fbm",
+               method = "em", control = list(stop.crit = 1e-3)))

## =====
## Converged after 65 iterations.
## Log-likelihood value: -204.4592
##
##      lambda      psi
## 3.24112 1869.32897

R> # Model 5: fBm RKHS (estimate Hurst)
R> (mod5 <- iprior(fat.train, absorp.train, kernel = "fbm", method = "mixed",
```



```
+             est.hurst = TRUE, control = list(stop.crit = 1e-3)))

## Running 5 initial EM iterations
## =====
## Now switching to direct optimisation
## iter    10 value 115.648462
## final   value 115.645800
## converged
## Log-likelihood value: -231.2923
##
##      lambda      hurst      psi
## 204.97184    0.70382    9.96498
```

Finally, we fit an I-prior model using the SE RKHS with lengthscale estimated. Here we illustrate the use of the `restarts` option, in which the model is fitted repeatedly from different starting points. In this case, eight random initial parameter values were used and these jobs were parallelised across the eight available cores of the machine. The additional `par.maxit` option in the `control` list is an option for the maximum number of iterations that each parallel job should do. We have set it to 100, which is the same number for `maxit`, but if `par.maxit` is less than `maxit`, the estimation procedure continues from the model with the best likelihood value. We see that starting from eight different initial values, direct optimisation leads to (at least) two log-likelihood optima sites, -231.5 and -680.5 .

```
R> # Model 6: SE kernel
R> (mod6 <- iprior(fat.train, absorp.train, est.lengthscale = TRUE,
+               kernel = "se", control = list(restarts = TRUE,
+               par.maxit = 100)))

## Performing 8 random restarts on 8 cores
## =====
## Log-likelihood from random starts:
##      Run 1      Run 2      Run 3      Run 4      Run 5      Run 6      Run 7
## -231.5440 -680.4636 -680.4636 -680.4637 -680.4637 -231.5440 -231.5440
## Continuing on Run 6
## final   value 115.771932
## converged
```

```
## Log-likelihood value: -231.544
```

```
##
```

```
##      lambda lengthscale      psi
```

```
##    96.11515      0.09269    6.15426
```

Predicted values of the test data set can be obtained using the `predict()` function. An example for obtaining the first model's predicted values is shown below. The `predict()` method for `ipriorMod` objects also return the test MSE if the vector of test data is supplied.

```
R> predict(mod1, newdata = list(absorp.test), y.test = fat.test)
```

```
## Test RMSE: 2.890353
```

```
##
```

```
## Predicted values:
```

```
## [1] 43.607 20.444 7.821 4.491 9.044 8.564 7.935 11.615 13.807
```

```
## [10] 17.359
```

```
## # ... with 33 more values
```

These results are summarised in [Table 4.5](#). For the I-prior models, a linear effect of the functional covariate gives a training RMSE of 2.89, which is improved by both the quadratic and cubic model. The training RMSE is improved further by assuming a smooth RKHS of functions for f , i.e. the fBm and SE RKHSs. When it comes to out-of-sample test error rates, the cubic model gives the best RMSE out of the I-prior models for this particular data set, with an RMSE of 0.58. This is followed closely by the fBm RKHS with estimated Hurst coefficient (fBm-0.70) and also the fBm RKHS with default Hurst coefficient (fBm-0.50). The best performing I-prior model is only outclassed by the neural networks of [Thodberg \(1996\)](#), who also performed model selection using automatic relevance determination (ARD). The I-prior models also give much better test RMSE than Gaussian process regression⁵.

⁵GPR models were fit using `gausspr()` in `kernlab`.

Table 4.5: A summary of the root mean squared error (RMSE) of prediction for the I-prior models and various other methods in literature conducted on the Tecator data set. Values for the methods under *Others* were obtained from the corresponding references cited earlier.

Model	RMSE	
	Train	Test
<i>I-prior</i>		
Linear	2.89	2.89
Quadratic	0.72	0.97
Cubic	0.37	0.58
Smooth (fBm-0.50)	0.00	0.68
Smooth (fBm-0.70)	0.19	0.63
Smooth (SE-0.09)	0.35	1.85
<i>Gaussian process regression</i>		
Linear	0.18	2.36
Smooth (SE-7.04)	0.17	2.10
<i>Others</i>		
Neural network ^a		0.36
Kernel smoothing ^b		1.49
Single/multiple indices model ^c		1.55
Sliced inverse regression		0.90
Sliced average variance estimation		1.70
MARS ^d		0.88
Partial least squares ^d		1.01
CSEFAM ^d		0.85

^a Neural network best results with automatic relevance determination (ARD) quoted.

^b Data set used was a 160/55 training/test split.

^c These are results of a leave-one-out cross-validation scheme.

^d Data set used was an extended version with $n = 240$, and a random 185/55 training/test split.

tab:tecator

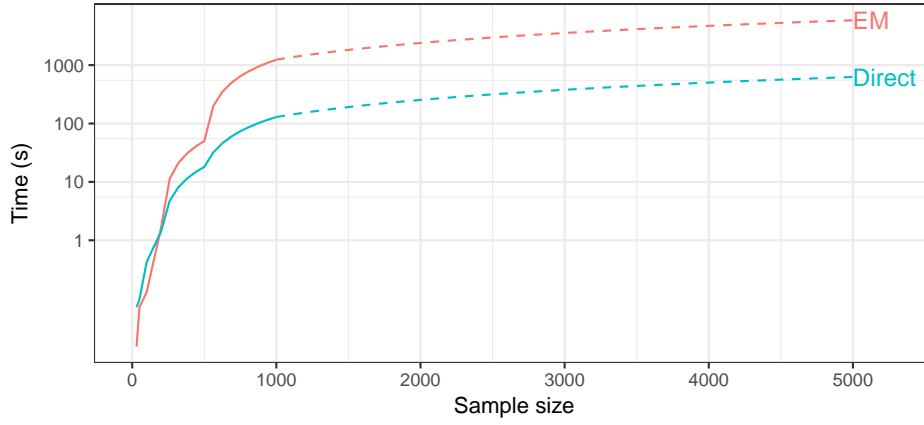


Figure 4.12: Average time taken to complete the estimation of an I-prior model (EM algorithm and direct optimisation) of varying sample sizes. The solid line represents actual timings, while the dotted lines are linear extrapolations.

fig:iprior
time

4.6 Conclusion

The steps for I-prior modelling are essentially three-fold:

1. Select an appropriate function space (equivalently, kernels) for which specific effects are desired on the covariates.
2. Estimate the posterior regression function and optimise the hyperparameters, which include the RKHS scale parameter(s), error precision, and any other kernel parameters such as the Hurst index.
3. Perform post-estimation procedures such as
 - Posterior predictive checks;
 - Model comparison via log-likelihood ratio tests/empirical Bayes factors; and
 - Prediction of new data point.

The main sticking point with the estimation procedure is the involvement of the $n \times n$ kernel matrix, for which its inverse is needed. This requires $O(n^2)$ storage and $O(n^3)$ computational time. The computational issue faced by I-priors are mirrored in Gaussian process regression, so the methods to overcome these computational challenges in GPR can be explored further. However, most efficient computational solutions exploit

the nature of the SE kernel structure, which is the most common kernel used in GPR. Nonetheless, we suggest the following as considerations for future work:

1. **Sparse variational approximations.** Variational methods have seen an active development in recent times. By using inducing points (Titsias, 2009) or stochastic variational inference (Hensman et al., 2013), such methods can greatly reduce computational storage and speed requirements. A recent paper by Cheng and Boots (2017) also suggests a variational algorithm with linear complexity for GPR-type models.
2. **Accelerating the EM algorithm.** Two methods can be explored. The first is called parameter-expansion EM algorithm (PXEM) by (Liu et al., 1998), which has been shown to be promising for random-effects type models. It involves correcting the M-step by a ‘covariance adjustment’, so that extra information can be capitalised on to improve convergence rates. The second is a quasi-Newton acceleration of the EM algorithm as proposed by Lange (1995). A slight change to the EM gradient algorithm in the M-step steers the EM algorithm to the Newton-Raphson algorithm, thus exploiting the benefits of the EM algorithm in the early stages (monotonic increase in likelihood) and avoiding the pitfalls of Newton-Raphson (getting stuck in local optima). Both algorithms require an in-depth reassessment of the EM algorithm to be tailored to I-prior models.

Bibliography

- bergsma2017 Bergsma, Wicher (2017). “Regression with I-priors”. In: *Unpublished manuscript*.
- carpenter2016stan Carpenter, Bob, Andrew Gelman, Matthew Hoffman, Daniel Lee, Ben Goodrich, Michael Betancourt, Marcus Brubaker, Jiqiang Guo, Peter Li, and Allen Riddell (2017). “Stan: A Probabilistic Programming Language”. In: *Journal of Statistical Software, Articles* 76.1, pp. 1–32. DOI: [10.18637/jss.v076.i01](https://doi.org/10.18637/jss.v076.i01).
- casella2002statistical Casella, George and Roger L Berger (2002). *Statistical inference*. Vol. 2. Duxbury Pacific Grove, CA.
- chen2011single Chen, Dong, Peter Hall, and Hans-Georg Müller (2011). “Single and Multiple Index Functional Regression Models with Nonparametric Link”. In: *The Annals of Statistics* 39.3, pp. 1720–1747. DOI: [10.1214/11-AOS882](https://doi.org/10.1214/11-AOS882).
- cheng2017variational Cheng, Ching-An and Byron Boots (2017). “Variational Inference for Gaussian Process Models with Linear Complexity”. In: *Advances in Neural Information Processing Systems*, pp. 5190–5200.
- davidian1995nonlinear Davidian, Marie and David M Giltinan (1995). *Nonlinear Models for Repeated Measurement Data*. Chapman and Hall/CRC.
- dempster1977maximum Dempster, Arthur P, Nan M Laird, and Donald B Rubin (1977). “Maximum likelihood from incomplete data via the EM algorithm”. In: *Journal of the royal statistical society. Series B (methodological)*, pp. 1–38.
- denwood2016runjags Denwood, Matthew (2016). “**runjags**: An R Package Providing Interface Utilities, Model Templates, Parallel Computing Methods and Additional Distributions for MCMC Models in JAGS”. In: *Journal of Statistical Software* 71.9, pp. 1–25. DOI: [10.18637/jss.v071.i09](https://doi.org/10.18637/jss.v071.i09).

ferraty2006 nonparametric	Ferraty, Frédéric and Philippe Vieu (2006). <i>Nonparametric Functional Data Analysis</i> . 1st. Springer-Verlag. DOI: 10.1007/0-387-36620-2 .
fowlkes2001 efficient	Fowlkes, C, S Belongie, and J Malik (2001). “Efficient Spatiotemporal Grouping Using the Nyström Method”. In: <i>Proceedings of the 2001 IEEE Computer Society Conference on Computer Vision and Pattern Recognition (CVPR 2001)</i> . Vol. 1, pp. 231–238. DOI: 10.1109/CVPR.2001.990481 .
hensman2013 gaussian	Hensman, James, Nicolo Fusi, and Neil D Lawrence (2013). “Gaussian processes for big data”. In: <i>arXiv preprint arXiv:1309.6835</i> .
jamil2017	Jamil, Haziq and Wicher Bergsma (2017). “iprior: An R Package for Regression Modelling using I-priors”. In: <i>Manuscript in submission</i> .
kenward1987 method	Kenward, Michael G. (1987). “A Method for Comparing Profiles of Repeated Measurements”. In: <i>Journal of the Royal Statistical Society C (Applied Statistics)</i> 36.3, pp. 296–308. DOI: 10.2307/2347788 .
caret	Kuhn, Max et al. (2017). caret : <i>Classification and Regression Training</i> . R package version 6.0–77. URL: https://CRAN.R-project.org/package=caret .
lange1995quasi	Lange, Kenneth (1995). “A quasi-Newton acceleration of the EM algorithm”. In: <i>Statistica sinica</i> , pp. 1–18.
lian2014series	Lian, Heng and Gaorong Li (2014). “Series Expansion for Functional Sufficient Dimension Reduction”. In: <i>Journal of Multivariate Analysis</i> 124.C, pp. 150–165. DOI: 10.1016/j.jmva.2013.10.019 .
liu1998parameter	Liu, Chuanhai, Donald B Rubin, and Ying Nian Wu (1998). “Parameter expansion to accelerate EM: The PX-EM algorithm”. In: <i>Biometrika</i> 85.4, pp. 755–770.
lunn2000winbugs	Lunn, David J., Andrew Thomas, Nicky Best, and David Spiegelhalter (Oct. 2000). “WinBUGS - A Bayesian modelling framework: Concepts, structure, and extensibility”. In: <i>Statistics and Computing</i> 10.4, pp. 325–337. DOI: 10.1023/A:1008929526011 .
meng1993maximum	Meng, Xiao-Li and Donald B Rubin (1993). “Maximum likelihood estimation via the ECM algorithm: A general framework”. In: <i>Biometrika</i> 80.2, pp. 267–278.
jmcm	Pan, Jianxin and Yi Pan (2016). jmcm : <i>Joint Mean-Covariance Models using Armadillo and S4</i> . R package version 0.1.7.0. URL: https://CRAN.R-project.org/package=jmcm .

pinheiro2000mixed	Pinheiro, José C and Douglas M Bates (2000). <i>Mixed-Effects Models in S and S-plus</i> . Springer-Verlag. DOI: 10.1007/b98882 .
nlme	Pinheiro, Joséo, Douglas Bates, Saikat DebRoy, Deepayan Sarkar, and R Core Team (2017). nlme : <i>Linear and Nonlinear Mixed Effects Models</i> . R package version 3.1-131. URL: https://CRAN.R-project.org/package=nlme .
plummer2003jags	Plummer, Martyn (2003). “JAGS: A Program for Analysis of Bayesian Graphical Models Using Gibbs Sampling”. In: <i>Proceedings of the 3rd International Workshop on Distributed Statistical Computing</i> . Vol. 124. Vienna, Austria, p. 125.
quinonero2005unifying	Quiñonero-Candela, Joaquin and Carl Edward Rasmussen (Dec. 2005). “A Unifying View of Sparse Approximate Gaussian Process Regression”. In: <i>Journal of Machine Learning Research</i> 6, pp. 1939–1959.
rasmussen2006gaussian	Rasmussen, Carl Edward and Christopher K I Williams (2006). <i>Gaussian Processes for Machine Learning</i> . The MIT Press.
rstan	Stan Development Team (2016). RStan : <i>The R Interface to Stan</i> . R package version 2.14.1. URL: http://mc-stan.org/ .
sturtz2005r2winbugs	Sturtz, Sibylle, Uwe Ligges, and Andrew Gelman (2005). “ R2WinBUGS : A Package for Running WinBUGS from R”. In: <i>Journal of Statistical Software</i> 12.3, pp. 1–16. DOI: 10.18637/jss.v012.i03 .
thodberg1996review	Thodberg, Hans Henrik (1996). “A Review of Bayesian Neural Networks with an Application to near Infrared Spectroscopy”. In: <i>IEEE Transactions on Neural Networks</i> 7.1, pp. 56–72. DOI: 10.1109/72.478392 .
titsias2009variational	Titsias, Michalis (2009). “Variational learning of inducing variables in sparse Gaussian processes”. In: <i>Artificial Intelligence and Statistics</i> , pp. 567–574.
van2008reproducing	van der Vaart, Aad W and van Zanten (2008). “Reproducing kernel Hilbert spaces of Gaussian priors”. In: <i>Pushing the limits of contemporary statistics: contributions in honor of Jayanta K. Ghosh</i> . Institute of Mathematical Statistics, pp. 200–222.
wahba1990spline	Wahba, Grace (1990). <i>Spline models for observational data</i> . Vol. 59. Siam.
williams2001using	Williams, Christopher K I and Matthias Seeger (2001). “Using the Nyström Method to Speed Up Kernel Machines”. In: <i>Advances in Neural Information Processing Systems 13</i> . The MIT Press, pp. 682–688.

zellner1986
assessing

Zellner, Arnold (1986). “On assessing prior distributions and Bayesian regression analysis with g-prior distributions”. In: *Bayesian inference and decision techniques*.

zhu2014stru
ctured

Zhu, Hongxiao, Fang Yao, and Hao Helen Zhang (2014). “Structured Functional Additive Regression in Reproducing Kernel Hilbert Spaces”. In: *Journal of the Royal Statistical Society B (Statistical Methodology)* 76.3, pp. 581–603. DOI: [10.1111/rssb.12036](https://doi.org/10.1111/rssb.12036).